NASA Technical Memorandum 101622

Global/Local Stress Analysis of Composite Panels

J. B. Ransom and N. F. Knight, Jr.

June 1989

National Aeronautics and Space Administration

Langley Research Center
Hampton, Virginia 23665-5225

GLOBAL/LOCAL STRESS ANALYSIS OF COMPOSITE PANELS†

Jonathan B. Ransom‡ and Norman F. Knight, Jr.‡
NASA Langley Research Center
Hampton, Virginia

Abstract

A method for performing a global/local stress analysis is described and its capabilities are demonstrated. The method employs spline interpolation functions which satisfy the linear plate bending equation to determine displacements and rotations from a global model which are used as "boundary conditions" for the local model. Then, the local model is analyzed independent of the global model of the structure. This approach can be used to determine local, detailed stress states for specific structural regions using independent, refined local models which exploit information from less–refined global models. The method presented is not restricted to having a priori knowledge of the location of the regions requiring local detailed stress analysis. This approach also reduces the computational effort necessary to obtain the detailed stress state. Criteria for applying the method are developed. The effectiveness of the method is demonstrated using a classical stress concentration problem and a graphite–epoxy blade–stiffened panel with a discontinuous stiffener.

Nomenclature

$\mathbf{a}$	Vector of unknown spline coefficients of the interpolation function
a_i	Polynomial coefficients of the interpolation function, $i = 0, 1, \ldots, 9$
A	Cross–sectional area
A_{net}	Net cross–sectional area, $(W - 2r_0)h$
b	Stiffener spacing
D	Flexural rigidity
E	Young's modulus of elasticity
$\mathbf{f}$	Spline interpolation function
F_i	Natural logarithm coefficients of the interpolation function, $i = 1, 2, \ldots, n$
h	Panel thickness
h_s	Blade–stiffener height
K_t	Stress concentration factor, $\frac{(\sigma_x)_{max}}{(\sigma_x)_{nom}}$
l	Number of points on the local model boundary
L	Panel length
n	Number of points in the interpolation region

† Invited Talk at the Third Joint ASCE/ASME Mechanics Conference, University of California at San Diego, July 9 -12, 1989.

‡ Aerospace Engineer, Structural Mechanics Branch, Structural Mechanics Division.

N_x	Longitudinal stress resultant
$(N_x)_{avg}$	Average running load per inch
$(N_x)_{max}$	Maximum longitudinal stress resultant, $(\sigma_x)_{max}h$
$(N_x)_{nom}$	Nominal longitudinal stress resultant, $(\sigma_x)_{nom}h$
P	Applied load
q	Pressure loading on panel
r_0	Radius of the panel cutout
r_i	Radial coordinate of the i-th node in the interpolation region or along the local model boundary
R_I	Radius of the interpolation region
R_L	Radius of the circular local model
$\mathbf{S}$	Spline matrix
U_e	Element strain energy per unit area
$(U_e)_{max}$	Maximum element strain energy per unit area
W	Panel width
x_i	x coordinate of the i-th node in the interpolation region or along the local model boundary
y_i	y coordinate of the i-th node in the interpolation region or along the local model boundary
ε	Parameter used to facilitate spline matrix computation
$\Delta\sigma$	Change in stress
σ_x	Longitudinal stress
$(\sigma_x)_{max}$	Maximum longitudinal stress
$(\sigma_x)_{nom}$	Nominal longitudinal stress, $\frac{P}{A_{net}}$
Ω_{ij}	Natural logarithm terms of the spline matrix, $i,j = 1,2,\ldots,n$
∇^4	Biharmonic operator

Introduction

Discontinuities and eccentricities, which are common in practical structures, increase the difficulty in predicting accurately detailed local stress distributions, especially when the component is built of a composite material, such as a graphite–epoxy material. The use of composite materials in the design of aircraft structures introduces added complexity due to the nature of the material systems and the complexity of the failure modes. The design and certification process for aerospace structures requires an accurate stress analysis capability. Detailed stress analyses of complex aircraft structures and their subcomponents are required and can severely tax even today's computing resources. Embedding detailed "local" finite element models within a single "global" finite element model of an entire airframe structure is usually impractical due to the computational cost associated with the large number of degrees of freedom required for such a global detailed model. If the design load envelope of the structural component is extended, new regions with high stress gradients may be discovered. In that case,

the entire analysis with embedded local refinements may have to be repeated and thereby further reducing the practicality of this brute force approach for obtaining the detailed stress state.

The phrase global/local analysis has a myriad of definitions among analysts (*e.g.*, refs. [1,2]). The concept of global and local may change with every analysis level, and also from one analyst to another. An analyst may consider the entire aircraft structure to be the global model, and a fuselage section to be the local model. At another level, the fuselage or wing is the global model, and a stiffened panel is the local model. Laminate theory is used by some analysts to represent the global model, and micromechanics models are used for the local model. The global/local stress analysis methodology, herein, is defined as a procedure to determine local, detailed stress states for specific structural regions using information obtained from an independent global stress analysis. A separate refined local model is used for the detailed analysis. Global/local analysis research areas include such methods as substructuring, submodeling, exact zooming and hybrid techniques.

The substructuring technique is perhaps the most common technique for global/local analysis in that it reduces a complex structure to smaller, more manageable components, and simplifies the structural modeling (*e.g.*, refs. [3-5]). A specific region of the structure may be modeled by a substructure or multiple levels of substructures to determine the detailed response. Submodeling refers to any method that uses a node by node correspondence for the displacement field at the global/local interface boundary (*e.g.*, refs. [6-9]). A form of submodeling is used in reference [8] to perform a two–dimensional to three–dimensional global/local analysis. Recently, the specified boundary stiffness/force (SBSF) method [9] has been proposed as a global/local analysis procedure. This approach uses an independent subregion model with stiffnesses and forces as boundary terms. These stiffnesses and forces represent the effect of the rest of the structure upon the subregion. The stiffness terms are incorporated in the stiffness of the subregion model and the forces are applied on the boundary of the local model.

An efficient zooming technique , as described in reference [10], employs static condensation and exact structural reanalysis methods. Although this efficient zooming technique involves the solution of a system of equations of small order, all the previous refinement processes are needed to proceed to a new refinement level. An "exact" zooming technique [11] employs an expanded stiffness matrix approach rather than the reanalysis method described in reference [10]. The "exact" zooming technique utilizes results of only the previous level of refinement. For both methods, separate locally–refined subregion models are used to determine the detailed stress distribution in a known critical region. The subregion boundary is coincident with nodes

in the global model or the previously refined subregion model which is akin to the submodeling technique discussed earlier.

Hybrid techniques (*e.g.*, refs. [12,13]) make use of two or more methods in different domains of the structure. In the global variational methods, the domain of the governing equation is treated as a whole, and an approximate solution is constructed from a sequence of linearly independent functions (*i.e.*, Fourier series) that satisfy the geometric boundary conditions. In the finite element method, the domain is subdivided into small regions or elements within which approximating functions (usually low–order polynomials) are used to describe the continuum behavior. Global/local finite element analysis may refer to an analysis technique that simultaneously utilizes conventional finite element modeling around a local discontinuity with classical Rayleigh-Ritz approximations for the remainder of the structure. The computational effort is reduced as a result of the use of the limited number of finite element degrees of freedom; however, this approach presupposes that the analyst can identify an approximation sequence for the global behavior. The selection of this approximation sequence may, therefore, restrict this approach to regular geometries and specific boundary conditions.

The aforementioned global/local methods, with the exception of the submodeling technique, require that the analyst know where the critical region is located before performing the global analysis. However, a global/local methodology which does not require a priori knowledge of the location of the local region(s) requiring special modeling could offer advantages in many situations by providing the modeling flexibility required to address detailed local models as their need is identified.

The overall objective of the present study is to develop such a computational strategy for obtaining detailed stress states of composite structures. Specific objectives are:

1. To develop a method for performing global/local stress analysis of composite structures
2. To develop criteria for defining the global/local interface region and local modeling requirements
3. To demonstrate the computational strategy on representative structural analysis problems

The scope of the present study includes the global/local linear two–dimensional stress analysis of finite element structural models. The method developed is not restricted to having a priori knowledge of the location of the regions requiring detailed stress analysis. The guidelines for developing the computational strategy include the requirement that it be compatible with

general–purpose finite element computer codes, valid for a wide range of elements, extendible to geometrically nonlinear analysis, and cost–effective. In addition, the computational strategy should include a procedure for automatically identifying the critical region and defining the global/local interface region. Satisfying these guidelines will provide a general–purpose global/local computational strategy for use by the aerospace structural analysis community.

Global/Local Methodology

Global/local stress analysis methodology is defined as a procedure to determine local, detailed stress states for specific structural regions using information obtained from an independent global stress analysis. The local model refers to any structural subregion within the defined global model. The global stress analysis is performed independent of the local stress analysis. The interpolation region encompassing the critical region is specified. A surface spline interpolation function is evaluated at every point in the interpolation region yielding a spline matrix, $\mathbf{S}(x, y)$, and unknown coefficients, $\mathbf{a}$. The global field is used to compute the unknown coefficients. An independent, more refined local model is generated within the previously–defined interpolation region. The global displacement field is interpolated producing a local displacement field which is applied as a "boundary condition" on the boundary of the local model. Then, a complete two–dimensional local finite element analysis is performed.

The development of a global/local stress analysis capability for structures generally involves four key components. The first component is an "adequate" global analysis. In this context, "adequate" implies that the global structural behavior is accurately determined and that local structural details are at least grossly incorporated. The second component is a strategy for identifying, in the global model, regions requiring further study. The third component is a procedure for defining the "boundary conditions" along the global/local interface boundary. Finally, the fourth component is an "adequate" local analysis. In this context, "adequate" implies that the local detailed stress state is accurately determined and that compatibility requirements along the global/local interface are satisfied. The development of a global/local stress analysis methodology requires an understanding of each key component and insight into their interaction.

In practice, the global analysis model is "adequate" for the specified design load cases. However, these load cases frequently change in order to extend the operating region of the structure or to account for previously unknown affects. In these incidents, the global analysis may identify new "hot spots" that require further study. The methodology presented herein provides an analysis tool for these local analyses.

Terminology

The terminology of the global/local methodology presented herein is depicted in figure 1 to illustrate the components of the analysis procedure. The global model, figure 1a, is a finite element model of an entire structure or a subcomponent of a structure. A region requiring a more detailed interrogation is subsequently identified by the structural analyst. This region may be obvious, such as a region around a cutout in a panel, or not so obvious, such as a local buckled region of a curved panel loaded in compression. Because the location of these regions are usually unknown prior to performing the global analysis, the structural analyst must develop a global model with sufficient detail to represent the global behavior of the structure. An interpolation region is then identified around the critical region as indicated in figure 1b. An interpolation procedure is used to determine the displacements and rotations used as "boundary conditions" for the local model. The interpolation region is the region within which the generalized displacement solution will be used to define the interpolation matrix. The global/local interface boundary, indicated in figure 1c, coincides with the intersection of the boundary of the local model with the global model. The definition of the interface boundary may affect the accuracy of the interpolation and thus the local stress state. The local model lies within the interpolation region as shown in figure 1c and is generally more refined than the global model in order to predict more accurately the detailed state of stress in the critical region. However, the local model is independent of the global finite element model as indicated in figure 1d. The coordinates or nodes of the local model need not be coincident with any of the coordinates or nodes of the global model.

The global/local interpolation procedure consists of generating a matrix based on the global solution and a local interpolated field. The local interpolated field is that field which is interpolated from the global analysis and is valid over the domain of the local model. Local stress analysis involves the generation of the local finite element model, use of the interpolated field to impose boundary conditions on the local model, and the detailed stress analysis.

Global Modeling and Analysis

The development of a global finite element model of an aerospace structure for accurate stress predictions near local discontinuities is often too time consuming to impact the design and certification process. Predicting the global structural response of these structures often has many objectives including overall structural response, stress analysis, and determining internal load distributions. Frequently, structural discontinuities such as cutouts are only accounted for in

the overall sense. Any local behavior is then obtained by a local analysis, possibly by another analyst. The load distribution for the local region is obtained from the global analysis. The local model is then used to obtain the structural behavior in the specified region. For example, the global response of an aircraft wing is obtained by a coarse finite element analysis. A typical subcomponent of the wing is a stiffened panel with a cutout. Since cutouts are known to produce high stress gradients, the load distributions from the global analysis of the wing are applied to the stiffened panel to obtain the local detailed stress state. One difficulty in modeling cutouts is the need for the finite element mesh to transition from a circular pattern near the cutout to a rectangular pattern away from the cutout. This transition region is indicated in figure 2 and will be referred to as a transition square (*i.e.*, a square region around the cutout used to transition from rings of elements to a rectangular mesh). This transition modeling requirement impacts both the region near the cutout and the region away from the cutout. Near the cutout, quadrilateral elements may be skewed, tapered, and perhaps have an undesirable aspect ratio. In addition, as the mesh near the cutout is refined by adding radial "spokes" of nodes and "rings" of elements, the mesh away from the cutout also becomes refined. For example, adding radial spokes of nodes near the cutout also adds nodes and elements in the shaded regions (see figure 2) away from the cutout. This approach may dramatically increase the computational requirements necessary to obtain the detailed stress state. Alternate mesh generation techniques using transition zones of triangular elements or multipoint constraints may be used; however, the time spent by the structural analyst will increase substantially.

The global modeling herein, although coarse, is sufficient to represent the global structural behavior. The critical regions have been modeled with only enough detail to represent their effect on the global solution. This modeling step is one of the key components of the global/local methodology since it provides an "adequate" global analysis. Although the critical regions are known for the numerical studies discussed in a subsequent section, this a priori knowledge is not required but may be exploited by the analyst.

Local Modeling and Analysis

The local finite element modeling and analysis is performed to obtain a detailed analysis of the local structural region(s). The local model accurately represents the geometry of the structure necessary to provide the local behavior and stress state. The discretization requirements for the analysis are governed by the accuracy of the solution desired. The discretization of the local model is influenced by its proximity to a high stress gradient.

One approach for obtaining the detailed stress state is to model the local region with an arbitrarily large number of finite elements. Higher–order elements may be used to reduce the number of elements required. Detailed refinement is much more advantageous for use in the local model than in the global model. The local refinement affects only the local model, unlike embedding the same refinement in the global model which would propagate to regions not requiring such a level of detailed refinement. A second approach is to refine the model based on engineering judgement. Mesh grading, in which smaller elements are used near the gradient, may be used. An error measure based on the change in stresses from element to element may be used to determine the accuracy in the stress state obtained by the initial local finite element mesh. If the accuracy of the solution is not satisfactory, additional refinements are required. The additional refinements may be based on the coarse global model or the displacement field in the local model which suggests a third approach. The third approach is a multi–level global/local analysis. At the second local model level, any of the three approaches discussed may be used to obtain the desired local detailed stress state. Detailed refinement is used for local modeling in this study.

Global/Local Interface Boundary Definition

The definition of the global/local interface boundary is problem dependent. Herein, the location of the nodes on the interface boundary need not be coincident with any of the nodes in the coarse global model. Reference [7] concluded that the distance that the local model must extend away from a discontinuity is highly dependent upon the coarse model used. The more accurate the coarse model displacement field is, the closer the local model boundary may be to the discontinuity. This conclusion is based on the results of a study of a flat, isotropic panel with a central cutout subjected to uniform tension, but it extends to other structures with high stress gradients.

Stresses are generally obtained from a displacement–based finite element analysis by differentiation of the displacement field. For problems with stress gradients, the element stresses vary from element to element, and in some cases this change, $\Delta\sigma$, may be substantial. The change in stresses, $\Delta\sigma$, may be used as a measure of the adequacy of the finite element discretization. Large $\Delta\sigma$ values indicate structural regions where more modeling refinement is needed. Based on this method, structural regions with small values of $\Delta\sigma$ have obtained uniform stress states away from any gradients. Therefore, the global/local interface boundary should be defined in regions with small values of $\Delta\sigma$ (*i.e.*, away from a stress gradient). Exploratory

studies to define an automated procedure for selecting the global/local interface boundary have been performed using a measure of the strain energy. The strain energy per unit area is selected since it represents a combination of all the stress components instead of a single stress component. Regions with high stress gradients will also have changes in this measure of strain energy from element to element.

Global/Local Interpolation Procedure

The global/local analysis method is used to determine local, detailed stress states using independent, refined local models which exploit information from less refined global models. A two–dimensional finite element analysis of the global structure is performed to obtain its overall behavior. A critical region may be identified from the results of the global analysis. The global solution may be used to obtain an applied displacement field along the boundary (*i.e.*, boundary conditions) of an independent local model of the critical region. This step is one of the key components of the global/local methodology; namely, interpolation of the global solution to obtain boundary conditions for the local model.

Many interpolation methods are used to approximate functions (*e.g.*, ref. [14]). The interpolation problem may be stated as follows: given a set of function values $\mathbf{f}_i$ at n coordinates (x_i, y_i), determine a "best–fit" surface for these data. Mathematically, this problem can be stated as

$$[\mathbf{S}(x_i, y_i)] \begin{Bmatrix} \mathbf{a}_1 \\ \mathbf{a}_2 \\ \vdots \\ \mathbf{a}_n \end{Bmatrix} = \begin{Bmatrix} \mathbf{f}_1 \\ \mathbf{f}_2 \\ \vdots \\ \mathbf{f}_n \end{Bmatrix} \tag{1}$$

where $\mathbf{S}(x_i, y_i)$ is a matrix of interpolated functions evaluated at n points, the array $\mathbf{a}$ defines the unknown coefficients of the interpolation functions, and the array $\mathbf{f}$ consists of known values of the field being interpolated based on n points in the global model. Common interpolation methods include linear interpolation, Lagrangian interpolation and least–squares techniques for polynomial interpolation. Elementary linear interpolation is perhaps the simplest method and is an often used interpolation method in trigonometric and logarithmic tables. Another method is Lagrangian interpolation which is an extension of linear interpolation. For this method, data for n points are specified and a unique polynomial of degree $n - 1$ passing through the points can be determined. However, a more common method involving a least–squares polynomial fit minimizes the the sum of the square of the residuals. The drawbacks of least–squares polynomial fitting include the requirement for repeated solutions to minimize the sum of the residual, and

the development of an extremely ill–conditioned matrix of coefficients when the degree of the approximating polynomial is large. A major limitation of the approximating polynomials which fit a given set of function values is that they may be excessively oscillatory between the given points or nodes.

Mathematical Formulation of Spline Interpolation

Spline interpolation is a numerical analysis tool used to obtain the "best" local fit through a set of points. Spline functions are piecewise polynomials of degree m that are connected together at points called knots so as to have $m - 1$ continuous derivatives. The mathematical spline is analogous to the draftman's spline used to draw a smooth curve through a number of given points. The spline may be considered to be a perfectly elastic thin beam resting on simple supports at given points. A surface spline is used to interpolate a function of two variables and removes the restriction of single variable schemes which require a rectangular array of grid points. The derivation of the surface spline interpolation function used herein is based on the principle of minimum potential energy for linear plate bending theory. This approach incorporates a classical structural mechanics formulation into the spline interpolation procedure in a general sense. Using an interpolation function which also satisfies the linear plate bending equation provides inherent physical significance to a numerical analysis technique. The spline interpolation is used to interpolate the displacements and rotations from a global analysis and thereby provides a functional description of each field over the domain. The fields are interpolated separately which provides a consistent basis for interpolating global solutions based on a plate theory with shear flexibility effects incorporated. That is, the out–of–plane deflections and the bending rotations are interpolated independently rather than calculating the bending rotations by differentiating the interpolated out–of–plane deflection field.

The spline interpolation used herein is derived following the approach described by Harder and Desmairis in reference [15]. A spline surface is generated based on the solution to the linear isotropic plate bending equation

$$D\nabla^4 w = q. \tag{2}$$

Extensions have been made to the formulation presented in reference [15] to include higher–order polynomial terms (underlined terms in equation (3)). The extended Cartesian form which satisfies equation (2) is written as

$$f(x,y) = a_0 + a_1 x + a_2 y + \underline{a_3 x^2 + a_4 xy + a_5 y^2 + a_6 x^3 + a_7 x^2 y +}$$

$$\underline{a_8 xy^2 + a_9 y^3} + \sum_{i=1}^{n} F_i r_i^2 \ln(r_i^2) \tag{3}$$

where

$$r_i^2 = (x - x_i)^2 + (y - y_i)^2 \tag{4}$$

and x_i, y_i are the coordinates of the i-th node in the interpolation region. The higher–order polynomial terms were added to help represent a higher–order bending response than was being approximated by the natural logarithm term in the earlier formulation. The additional terms increase the number of unknown coefficients and constraint equations to $n + 10$. The $n + 10$ unknowns $(a_0, a_1, a_2, \ldots, a_9, F_i)$ are found from equation (3) and by solving the set of equations:

$$\begin{aligned}
\sum_{i=1}^{n} F_i &= 0 & \sum_{i=1}^{n} F_i y_i^2 &= 0 \\
\sum_{i=1}^{n} F_i x_i &= 0 & \sum_{i=1}^{n} F_i x_i^3 &= 0 \\
\sum_{i=1}^{n} F_i y_i &= 0 & \sum_{i=1}^{n} F_i x_i^2 y_i &= 0 \\
\sum_{i=1}^{n} F_i x_i^2 &= 0 & \sum_{i=1}^{n} F_i x_i y_i^2 &= 0 \\
\sum_{i=1}^{n} F_i x_i y_i &= 0 & \sum_{i=1}^{n} F_i y_i^3 &= 0
\end{aligned} \tag{5}$$

The constraint equations given in equation (5) are used to prevent equation (2) from becoming unbounded when expressed in Cartesian coordinates. The modified matrix equations, still of the

form $\mathbf{Sa} = \mathbf{f}$, are

$$\begin{bmatrix} 0 & 0 & 0 & \dots & 0 & 1 & 1 & \dots & 1 \\ 0 & 0 & 0 & \dots & 0 & x_1 & x_2 & \dots & x_n \\ 0 & 0 & 0 & \dots & 0 & y_1 & y_2 & \dots & y_n \\ 0 & 0 & 0 & \dots & 0 & x_1^2 & x_2^2 & \dots & x_n^2 \\ 0 & 0 & 0 & \dots & 0 & x_1y_1 & x_2y_2 & \dots & x_ny_n \\ 0 & 0 & 0 & \dots & 0 & y_1^2 & y_2^2 & \dots & y_n^2 \\ 0 & 0 & 0 & \dots & 0 & x_1^3 & x_2^3 & \dots & x_n^3 \\ 0 & 0 & 0 & \dots & 0 & x_1^2y_1 & x_2^2y_2 & \dots & x_n^2y_n \\ 0 & 0 & 0 & \dots & 0 & x_1y_1^2 & x_1y_2^2 & \dots & x_ny_n^2 \\ 0 & 0 & 0 & \dots & 0 & y_1^3 & y_2^3 & \dots & y_n^3 \\ 1 & x_1 & y_1 & \dots & y_1^3 & \Omega_{11} & \Omega_{12} & \dots & \Omega_{1n} \\ 1 & x_2 & y_2 & \dots & y_2^3 & \Omega_{21} & \Omega_{22} & \dots & \Omega_{2n} \\ \vdots & \vdots & \vdots & \ddots & \vdots & \vdots & \vdots & \vdots & \vdots \\ 1 & x_n & y_n & \dots & y_n^3 & \Omega_{n1} & \Omega_{n2} & \dots & \Omega_{nn} \end{bmatrix} \begin{Bmatrix} a_0 \\ a_1 \\ a_2 \\ a_3 \\ a_4 \\ a_5 \\ a_6 \\ a_7 \\ a_8 \\ a_9 \\ F_1 \\ F_2 \\ \vdots \\ F_n \end{Bmatrix} = \begin{Bmatrix} 0 \\ 0 \\ 0 \\ 0 \\ 0 \\ 0 \\ 0 \\ 0 \\ 0 \\ 0 \\ f_1 \\ f_2 \\ \vdots \\ f_n \end{Bmatrix} \tag{6}$$

where $\Omega_{ij} = r_{ij}^2 \ln(r_{ij}^2 + \varepsilon)$ for $i, j = 1, 2, \dots, n$ and ε is a parameter used to insure numerical stability for the case when r_{ij} vanishes. The extended local interpolation function is similar to equation (3) except that it is evaluated at points along the global/local interface boundary. That is,

$$f_i = a_0 + a_1x_i + a_2y_i + a_3{x_i}^2 + a_4x_iy_i + a_5{y_i}^2 + a_6{x_i}^3 + a_7{x_i}^2y_i +$$

$$a_8x_i{y_i}^2 + a_9{y_i}^3 + \sum_{j=1}^{n} F_j r_{ij}^2 \ln(r_{ij}^2); \qquad i = 1, 2, \dots, l \tag{7}$$

Upon solving equation (6) for the coefficients $(a_0, a_1, a_2, \dots, a_9, F_j)$, equation (7) is used to compute the interpolated data at the required local model nodes.

Computational Strategy

A schematic which describes the overall solution strategy is shown in figure 3. The computational strategy described herein is implemented through the use of the Computational Structural Mechanics (CSM) Testbed (see refs. [16] and [17]). The CSM Testbed is used to model and analyze both the global and local finite element models of a structure. Two computational modules or processors were developed to perform the global/local interpolation procedure. Processor SPLN evaluates the spline coefficient matrix $[\mathbf{S}(x_i, y_i)]$. Processor INTS solves for the interpolation coefficients $\mathbf{a} = \{a_i\ F_i\}$ and performs the local interpolation to obtain the "boundary conditions" for the local model. Various other Testbed processors are used in the

stress analysis procedure. The overall computational strategy for the global/local stress analysis methodology is controlled by a high–level procedure written using the command language of the Testbed (see ref. [17]). The command language provides a flexible tool for performing computational structural mechanics research.

Numerical Results

The effectiveness of the computational strategy for the global/local stress analysis outlined in the previous sections is demonstrated by obtaining the detailed stress states for an isotropic panel with a cutout and a blade–stiffened graphite epoxy panel with a discontinuous stiffener. The first problem was selected to verify the global/local analysis capabilities while the second problem was selected to demonstrate its use on a representative aircraft subcomponent. The objectives of these numerical studies are:

1. To demonstrate the global/local stress analysis methodology, and
2. To obtain and interrogate the detailed stress states of representative subcomponents of complete aerospace structures.

All numerical studies were performed on a Convex C220 minisupercomputer. The computational effort of each analysis is quantified by the number of degrees of freedom used in the finite element model, the computational time required to perform a stress analysis, and the amount of auxiliary storage required. The computational time is measured in central processing unit (CPU) time. The amount of auxiliary storage required is measured by the size of the data library used for the input/output of information to a disk during a Testbed execution.

Isotropic Panel with Circular Cutout

An isotropic panel with a cutout is an ideal structure to verify the global/local computational strategy, since closed–form elasticity solutions are available. Elasticity solutions for an infinite isotropic panel with a circular cutout (*e.g.*, ref. [18]), predict a stress concentration factor of three at the edge of the cutout. The influence of finite–width effects on the stress concentration factors for isotropic panels with cutouts are reported in reference [19]. By including finite–width effects, the stress concentration factor is reduced from the value of three for an infinite panel.

The global/local linear stress analysis of the isotropic panel with a circular cutout shown in figure 4 has been performed. The overall panel length L is 20 in., the overall width W is

10 in., the thickness h is .1 in, and the cutout radius r_0 is 0.25 in. This geometry gives a cutout diameter to panel width ratio of 0.05 which corresponds to a stress concentration factor of 2.85 (see ref. [19]). The loading is uniform axial tension with the loaded ends of the panel clamped and the sides free. The material system for the panel is aluminum with a Young's modulus of 10,000 ksi and Poisson's ratio of 0.3.

Global Analysis

The finite element model shown in figure 4 of the isotropic panel with a circular cutout is a representative finite element model for representing the global behavior of the panel as well as a good approximation to the local behavior. The finite element model shown in figure 4, will be referred to as the "coarse" global model or Model G1 in Table 1. The finite element model has a total of 256 4-node quadrilateral elements, 296 nodes, and 1644 active degrees of freedom for the linear stress analysis. This quadrilateral element corresponds to a flat C^1 shell element which is based on a displacement formulation and includes rotation about the outward normal axis. Originally developed for the computer code STAGS (see refs. [20,21]), this element has been installed in the CSM Testbed software system and denoted ES5/E410 (see ref. [16]).

The longitudinal stress resultant N_x distribution shown in figure 5 reveals several features of the global structural behavior of this panel. First, away from the cutout, the N_x distribution in the panel is uniform. Secondly, the N_x load near the center of the panel is much greater than the N_x load in other portions of the panel due to the redistribution of the N_x load as a result of the cutout. Thirdly, the N_x load at the edge of the cutout at the points ninety degrees away from the stress concentration is small relative to the uniform far–field stress state.

The distribution of the longitudinal stress resultant N_x at the panel midlength normalized by the nominal stress resultant is shown in figure 6 as a function of the distance from the cutout normalized by the cutout radius. The results indicate that high inplane stresses and a high gradient exist near the cutout. However, a stress concentration factor of 2.06 is obtained from a linear stress analysis using the "coarse" finite element model (see figure 4). This value is 28% lower than the theoretical value of 2.85 reported in reference [19]. Therefore, even though the overall global response of the panel is qualitatively correct as indicated by the stress resultant contour in figures 5, the detailed stress state near the discontinuity is inaccurate.

Accurate detailed stress distributions require a finite element mesh that is substantially more refined near the cutout. Adding only rings of elements (Model G2 in Table 1) does not affect the discretization away from the cutout; however, the stress concentration factor is still 22% lower

than the theoretical value. To obtain a converged solution for the stress concentration factor, a sequence of successively refined finite element models were developed by increasing the number of radial spokes of nodes and rings of elements in the region around the cutout. A converged solution is obtained using a total of 3168 4-node quadrilateral shell elements (ES5/E410) in the global model (Model G4 in Table 1). Using an intermediate refined finite element model with a total of 832 4-node quadrilateral elements, 888 nodes, and 5156 active degrees of freedom, a stress concentration factor of 2.72 is obtained which is within 4.6% of the theoretical solution. This finite element model is referred to as the "refined" global model or Model G3 in Table 1. Normalized longitudinal stress resultant N_x distributions are shown in figure 6 for the "coarse" global model (G1) and the "refined" global model (G3). The stress gradient for this panel becomes nearly zero at a distance from the center of the panel of approximately six times the cutout radius.

The distribution of the strain energy for Model G1 is shown in figure 7. The change in the strain energy per unit area within the transition square indicates that a high stress gradient exists near the cutout and rapidly decays away from the cutout. These results are consistent with the structural analyst's intuition, and the local analyses described subsequently will further interrogate the region near the cutout.

Local Analyses

A global/local analysis capability provides an alternative to global mesh refinement and a complete solution using a more refined mesh. For this example, the "critical" region is well known and easily identified by even a casual examination of the stress resultant distributions given in figure 5. The global model, the interpolation region and the local models considered are shown in figure 8. The global model corresponds to the "coarse" global model (G1) and the shaded region corresponds to the interpolation region which is used to generate the spline coefficient matrix and to extract boundary conditions for the local model. As indicated in figure 8, two different local models are considered: one square and one circular. Both local models completely include the critical region with the stress concentration. The boundary of the square local model coincides with the boundary of the transition square in the global model. The boundary of the circular model is inscribed in the transition square. That is, the outer radius of the circular model is equal to half the length of a side of the transition square. Both local models (Models LS1 and LC1 in Table 1) have the same number of 4-node quadrilateral shell elements (512), number of nodes (544) and number of degrees of freedom (3072). Both local models have only 62% of the elements used in the refined global analysis. The global/local interpolation for

both local models is performed from the data obtained from the "coarse" global model analysis. The radius of the interpolation region R_I is $5.7r_0$ which includes the 48 data points within the transition square of the coarse global model.

The distribution of the longitudinal stress resultant N_x at the panel midlength normalized by the nominal stress resultant obtained using the square local model is shown in figure 9a as a function of distance from the cutout normalized by the cutout radius. These results indicate that the global/local analysis based on the coarse global solution and the square local model accurately predicts the stress concentration factor at the cutout as well as the distribution at the global/local interface boundary. A stress concentration factor of 2.76 is obtained which is within 1.5% of the "refined" global model (G3) solution and 3.2% of the theoretical solution. A contour plot of the longitudinal stress resultant distribution is given in figure 9b and indicates that the local solution correlates well overall with the global solution shown in figure 5.

The distribution of the longitudinal stress resultant N_x at the panel midlength normalized by the nominal stress resultant obtained using the circular local model is shown in figure 10a as a function of distance from the cutout normalized by the cutout radius. These results indicate that the global/local analysis based on the coarse global solution and the circular local model accurately predicts the stress concentration factor at the cutout. A stress concentration factor of 2.75 is obtained which is within 1.5% of the "refined" global model (G3) solution and 3.2% of the theoretical solution. At the global/local interface boundary, the results from the circular local model differ slightly from the results obtained from the refined global model analysis. This difference is attributed to interaction between the "coarse" global model, the interpolation region, and the location of the global/local interface boundary. A contour plot of the longitudinal stress resultant distribution is given in figure 10b and indicates the overall correlation with the distributions obtained using the global models.

The interaction between the global model, the interpolation region, and the location of the global/local interface boundary is now assessed. This assessment involves refining the global model in the transition square, varying the radius of the interpolation region R_I and varying the radius of the local model R_L. Using an interpolation region defined as $R_I = 14r_0$ (72 data points from the global model), several local models are considered in which R_L is increased from twice the cutout radius to five times the cutout radius. The results in figure 11a are based on using the coarse global model (G1) for the global solution. These results indicate that the local solution deteriorates as the global/local interface boundary is moved closer to the cutout. The results in figure 11b are based on a slightly more refined global model(G2) for the global solution.

This global model has two additional rings of elements in the transition square. Comparing the results in figures 11a and 11b reveals the interaction between the global model and the location of the interface boundary. To obtain an accurate local solution for the case when the global/local interface boundary is located within a region with a high stress gradient requires that sufficient data from the global model be available in the area to provide accurate "boundary conditions" for the local model. These results indicate that by adding just two rings of elements near the cutout (Model G2), the extraction of the local model boundary conditions from the spline interpolation is improved such that the global/local interface boundary may be located very near the cutout.

The influence of the radius of the interpolation region on the local solution was determined to be minimal provided the global model discretization is adequate. For the cases considered, identical local solutions are obtained using an interpolation region larger than the local model or an interpolation region which coincides with the local model.

Computational Requirements

A summary of the computational requirements for the global and local analyses of the isotropic panel with the circular cutout is given in Table 2. The computational cost in central processing unit (CPU) seconds of the local analyses is approximately 74% of the CPU time of the refined global analysis. The CSM Testbed data libraries for the local analyses are 59% smaller than the data library for the refined global analysis. The local models have 60% and 16% of the total number of degrees of freedom required for the refined model (G3) and converged global model (G4), respectively.

Usage Guidelines

Usage guidelines derived from the global/local analysis of the isotropic panel with a circular cutout are as follows. An "adequate" global analysis is required to ensure a sufficient number of accurate data points to provide accurate "boundary conditions" for the local model. When the global/local interface boundary, R_L is within the high stress gradient (*i.e.*, within a distance of two times the cutout radius from the cutout edge), the importance of an "adequate" global analysis in the high gradient region is increased. The interpolation region should coincide with or be larger than the local model. To satisfy the compatibility requirements at the global/local interface boundary, the local model boundary R_L should be defined sufficiently far from the cutout (*i.e.*, a distance of approximately six times the radius from the cutout).

Composite Blade–Stiffened Panel with Discontinuous Stiffener

Discontinuities and eccentricities are common in aircraft structures. For example, the lower surface of the Bell–Boeing V-22 tilt–rotor wing structure has numerous cutouts and discontinuous stiffeners (see figure 12). Predicting the structural response of such structures in the presence of discontinuities, eccentricities, and damage is particularly difficult when the component is built from graphite–epoxy materials or is loaded into the nonlinear range. In addition, potential damage of otherwise perfect structures is often an important design consideration. Recent interest in applying graphite–epoxy materials to aircraft primary structures has led to several studies of postbuckling behavior and failure characteristics of graphite–epoxy components (*e.g.*, ref. [22]). One goal of these studies has been the accurate prediction of the global response of the composite structural component in the postbuckling range. In one study of composite stiffened panels, a blade–stiffened panel was tested (see ref. [23]). A composite blade–stiffened panel was proof-tested and used as a "control specimen". The panel was subsequently used in a study on discontinuities in composite blade–stiffened panels. The global structural response of these composite blade–stiffened panels presented in reference [24] correlate well with the earlier experiment data. The composite blade–stiffened panel with a discontinuous stiffener shown in figure 13 is representative of an typical aircraft structural component and will be used to demonstrate and assess the global/local methodology. This problem was selected because it has characteristics which often require a global/local analysis. These characteristics include a discontinuity, eccentric loading, large displacements, large stress gradients, high inplane loading, and a brittle material system. This problem represents a generic class of laminated composite structures with discontinuities for which the interlaminar stress state becomes important. The local and global finite element modeling and analysis needed to predict accurately the detailed stress state of flat blade–stiffened graphite–epoxy panels loaded in axial compression is described in this section.

The overall panel length L is 30 in., the overall width W is 11.5 in., the stiffener spacing b is 4.5 in., the stiffener height h_s is 1.4 in., and the cutout radius r_0 is 1 in. The three blade–shaped stiffeners are identical. The loading is uniform axial compression. The loaded ends of the panel are clamped and the sides are free. The material system for the panel is T300/5208 graphite–epoxy unidirectional tapes with a nominal ply thickness of 0.0055 in. Typical lamina properties for this graphite–epoxy system are 19,000 ksi for the longitudinal Young's modulus, 1,890 ksi for the transverse Young's modulus, 930 ksi for the shear modulus, and 0.38 for the major Poisson's

ratio. The panel skin is a 25-ply laminate $([\pm 45/0_2/\mp 45/0_3/\pm 45/0_3/\mp 45/0_3/\pm 45/0_2/\mp 45])$ and the blade stiffeners are 24-ply laminates $([\pm 45/0_{20}/\mp 45])$.

End–shortening results are shown in figure 14 for the "control specimen" and for the configuration with a discontinuous stiffener. These results indicate that the presence of the discontinuity markedly changes the structural response of the panel. The structural response of the "control specimen" is typical of stiffened panels. Two equilibrium configurations are exhibited; namely, the prebuckling configuration and the postbuckling configuration. The structural response of the configuration with a discontinuous stiffener is nonlinear from the onset of loading due to the eccentric loading condition and the cutout. The blade–stiffened panel with a discontinuous stiffener was tested to failure. Local failures occurred prior to overall panel failure as evident from the end–shortening results shown in figure 14.

Global Analysis

A global linear stress analysis of the composite blade–stiffened panel with a discontinuous stiffener was performed for an applied load corresponding to P/EA of 0.0008 (*i.e.*, an applied compressive load P of 19,280 pounds normalized by the extensional stiffness EA). At this load level, the structural response of the panel is essentially linear. Out–of–plane deflections are present, however, due to the eccentric loading condition caused by the discontinuous stiffener. Several global finite element models are considered as indicated in Table 3 to obtain a converged solution for comparison purposes since a theoretical solution is not available. The value of the longitudinal stress resultant at the edge of the cutout changed less than 2% between Models G2 and G4. Therefore, Model G1 will be referred to as the "coarse" global model (see figure 15), Model G2 will be referred to as the "refined" global model, and Model G4 will be referred to as the "converged" global model.

The distribution of the longitudinal stress resultant N_x normalized by the average applied running load $(N_x)_{avg}$ (*i.e.*, applied load divided by the panel width) as a function of the lateral distance from the center of the panel normalized by the radius of the cutout is shown in figure 16 for both the "coarse" (G1) and the "refined" (G2) global models. These results are similar to those obtained for the isotropic panel with a cutout. The maximum longitudinal stress resultants $(N_x)_{max}$ normalized by the average applied running load $(N_x)_{avg}$ are given in Table 3. The results obtained using the coarse global model adequately represent the distribution away from the discontinuity but underestimate (by 24%) the stress concentration at the edge of the discontinuity.

An oblique view of the deformed shape with exaggerated deflections is shown in figure 17 for the coarse global model. A contour plot of the longitudinal inplane stress resultant N_x is also shown in this figure. The distribution indicates that the model provides good overall structural response characteristics. The N_x distribution reveals several features of the global structural behavior of this panel. First, away from the discontinuity, the N_x distribution in the panel skin is nearly uniform and approximately half the value of the N_x in the outer two blade stiffeners. Second, load is diffused from the center discontinuous stiffener into the panel skin rapidly such that the center stiffener has essentially no N_x load at the edge of the cutout. Third, the N_x load in the outer stiffeners increases towards the center of the panel and is concentrated in the blade free edges (*i.e.*, away from the stiffener attachment line at the panel skin). Fourth, the N_x load in the panel skin near the center of the panel is much greater than the N_x load in other portions of the panel skin.

The distribution of the strain energy for Model G1 is shown in figure 18. The change in the strain energy per unit area within the transition square again indicates that a high stress gradient exists near the discontinuity and rapidly decays away from the discontinuity. These results are consistent with the structural analyst's intuition, and the local models described subsequently will further interrogate the region near the discontinuity. For this load level, the skin–stiffener interface region has not yet become heavily loaded. However, this region will also be studied further to demonstrate the flexibility of the global/local stress analysis procedure presented herein.

Local Analyses

A global/local analysis capability provides an alternative approach to global mesh refinement and a complete solution using a more refined mesh. For this example, one "critical" region is easily identified by even a casual examination of the stress resultant distribution given in figure 17. A second critical region that may require further study is indicated by the slight gradient near the intersection of the outer blade–stiffeners and the panel skin at the panel midlength as shown in figure 17. Skin–stiffener separation has been identified as a dominant failure mode for stiffened composite panels (see ref. [22]). The global model, the interpolation regions and the local models considered are shown in figure 19. The global model corresponds to the "coarse" global model (G1) and the shaded regions correspond to the interpolation regions which are used to generate the spline coefficient matrix and to extract boundary conditions for the local model. As indicated in figure 19, two different critical regions are considered. One region is near the discontinuity and a circular local model is used. The boundary of the circular

model is inscribed in the transition square. That is, the outer radius of the circular model is equal to half the length of a side of the transition square. The other region is near the skin–stiffener interface region at the panel midlength for one of the outer stiffeners. The global/local interpolation for the local models is performed from the data obtained from the "coarse" global model analysis. Two interpolation regions were used in each of the local analyses. The first interpolation region, specified in the plane of the panel skin, is used to obtain the boundary conditions on the global/local interface boundary of the panel skin. The second interpolation region, specified in the plane of the stiffener, is used to obtain the boundary conditions on the global/local interface boundary of the stiffener. The boundary conditions for the panel skin and the stiffener were interpolated separately. Compatibility of displacements and rotations at the skin–stiffener intersection on the global/local interface boundaries was enforced by imposing the boundary conditions obtained for the panel skin.

The local model (Model LC1 in Table 3) of the first critical region near the discontinuity has 576 4-node quadrilateral shell elements, 612 nodes, and 3456 degrees of freedom. This local model has only 56% of the elements used in the refined global analysis. The distribution of the longitudinal stress resultant N_x at the panel midlength normalized by the average running load $(N_x)_{avg}$ is shown in figure 20a as a function of the lateral distance from the cutout normalized by the cutout radius. These results indicate that the global/local analysis based on the coarse global solution accurately predicts the stress concentration at the cutout as well as the distribution at the global/local interface boundary. A contour plot of the longitudinal stress resultant distribution is given in figure 20b. The results indicate that the local solution correlates well with the global solutions shown in figure 17.

The second critical region near the intersection of the outer blade–stiffener and the panel skin at the midlength is studied further. Three different local finite element models of this critical region are considered as indicated in Table 3. The first, Model LR1, has the same number of nodes (25) and number of elements (16) within the critical region as the coarse global model (G1). The second, Model LR2, has the same number of nodes (45) and number of elements (32) within the critical region as the refined global model (G2). The third and most refined model, Model LR3, has 117 nodes, 96 elements and 462 degrees of freedom. The longitudinal stress resultant N_x distributions obtained for the local models (LR1 and LR2) correlate well with the N_x distributions for the coarse and refined global models (Models G1 and G2). However, these models are not sufficiently refined in the skin–stiffener interface region to accurately predict the gradient at the skin–stiffener intersection. The distribution of the longitudinal stress resultant

N_x normalized by the applied running load as a function of the lateral distance from the center of the panel normalized by the radius of the cutout is shown in figure 21. These results indicate that the global/local analysis using the local model Model LR3 predicts a higher gradient at $\frac{y}{r_0} = -4.5$ in the skin–stiffener interface region than the other global and local analyses. A third global model Model G3 is used to investigate the local structural behavior predicted by Model LR3. The global analysis performed with Model G3 predicts the same local behavior as the analysis performed with Model LR3 as indicated in figure 21. Several factors should be borne in mind. First, the local analysis revealed local behavior at the skin–stiffener interface region that was not predicted by either of the global models. Second, the global modeling requirement for examining the skin–stiffener interface region are substantial. Because the global models were generated to predict the stress distribution around the discontinuity, additional radial "spokes" in the transition square are required to refine the panel skin in the skin–stiffener interface region in the longitudinal direction. Third, the global/local analysis capability provides the analyst with the added modeling flexibility to obtain an accurate detailed response at multiple critical regions (*i.e.*, at the discontinuity and at the skin–stiffener interface region) with minimal modeling and computational effort.

Computational Requirements

A summary of the computational requirements for the global and local analyses of the graphite–epoxy blade–stiffened panel with the discontinuous stiffener is given in Table 4. The computational cost in CPU seconds of the local analyses around the discontinuity is approximately 57% of the CPU time of the refined global analysis. The CSM Testbed data libraries for the local analyses are half of the size of the data library for the refined global analysis. The local models have 55% and 16% of the total number of degrees of freedom required for the refined model (G2) and converged global model (G4), respectively. The CPU time for the refined local analysis (LR3) of the skin–stiffener interface region is 24% of the CPU time required for the global analysis with Model G3. The size of the data library for the local analysis is 5% of the size of the data library required for the analysis with Model G3.

Usage Guidelines

Usage guidelines derived from the global/local analysis of the blade–stiffened panel with a discontinuous stiffener are as follows. An "adequate" global analysis is required to ensure a sufficient number of accurate data points to provide accurate "boundary conditions" for the local model. When the global/local interface boundary, R_L is within the high stress gradient

(*i.e.*, within a distance of two times the cutout radius from the cutout edge), the importance of an "adequate" global analysis in the high gradient region is increased. The interpolation region should coincide with or be larger than the local model. To satisfy the compatibility requirements at the global/local interface boundary, the local model boundary R_L should be defined sufficiently far from the cutout (*i.e.*, a distance of approximately six times the radius from the cutout). For the blade–stiffened panel, two interpolation regions should be specified, one for the interpolation of the boundary conditions on the boundary of the panel skin and a second for the interpolation of the boundary conditions on the outer edges of the stiffeners.

Conclusions

A global/local analysis methodology for obtaining the detailed stress state of structural components is presented. The methodology presented is not restricted to having a priori knowledge of the location of the regions requiring a detailed stress analysis. The effectiveness of the global/local analysis capability is demonstrated by obtaining the detailed stress states of an isotropic panel with a cutout and a blade–stiffened graphite–epoxy panel with a discontinuous stiffener.

Although the representative global finite element models represent the global behavior of the structures, substantially more refined finite element meshes near the cutouts are required to obtain accurate detailed stress distributions. Embedding a local refined model in the complete structural model increases the computational requirements. The computational effort for the independent local analyses is less than the computational effort for the global analyses with the embedded local refinement.

The global/local analysis capability provides the modeling flexibility required to address detailed local models as their need arises. This modeling flexibility was demonstrated by the local analysis of the skin–stiffener interface regions of the blade–stiffened panel with a discontinuous stiffener. This local analysis revealed local behavior that was not predicted by the global analysis.

The definition of the global/local interface boundary affects the accuracy of the local detailed stress state. The strain energy per unit area has been identified as a means for identifying a critical region and the location of the associated global/local interface boundary. The change in strain energy from element to element indicates regions with high stress gradients (*i.e.*, critical regions). A global/local interface boundary is defined outside of a region with large changes in strain energy.

The global/local analysis capability presented provides a general–purpose analysis tool for use by the aerospace structural analysis community by providing an efficient strategy for accurately predicting local detailed stress states that occur in structures discretized with relatively coarse finite element models. The coarse model represents the global structural behavior and approximates the local stress state. Independent, locally–refined finite element models are used to accurately predict the detailed stress state in the regions of interest based on the solution predicted by the coarse global analysis.

Acknowledgements

This work represents a portion of the first author's Master's thesis submitted to the faculty of the Old Dominion University.

References

1. Knight, Norman F., Jr.; Greene, William H.; and Stroud, W. Jefferson: Nonlinear Response of a Blade–Stiffened Graphite–Epoxy Panel with a Discontinuous Stiffener. Proceedings of NASA Workshop on Computational Methods in Structural Mechanics and Dynamics, W. J. Stroud; J. M. Housner; J. A. Tanner; and R. J. Hayduk (editors), June 19-21, 1985, NASA CP–3034 - PART 1, 1989, pp. 51-66.

2. Noor, Ahmed K.: Global–Local Methodologies and Their Application to Nonlinear Analysis. Finite Elements in Analysis and Design, Vol. 2, No. 4, December 1986, pp. 333-346.

3. Wilkins, D. J.: A Preliminary Damage Tolerance Methodology for Composite Structures. Proceedings of NASA Workshop on Failure Analysis and Mechanisms of Failure of Fibrous Composite Structures, A. K. Noor, M. J. Shuart, J. H. Starnes, Jr., and J. G. Williams (compilers), NASA CP–2278, 1983, pp. 61-93.

4. Han, Tao-Yang; and Abel, J. F.: Computational Strategies for Nonlinear and Fracture Mechanics, Adaptive Substructuring Techniques in Elasto–Plastic Finite Element Analysis. Computers and Structures, Vol. 20, No. 1-3, 1985, pp. 181-192.

5. Clough, R. W.; and Wilson, E. L.: Dynamic Analysis of Large Structural Systems with Local Nonlinearities. Computer Methods in Applied Mechanics and Engineering, Vol. 17/18, Part 1, January 1979, pp. 107-129.

6. Schwartz, David J.: Practical Analysis of Stress Raisers in Solid Structures. Proceedings of the 4th International Conference on Vehicle Structural Mechanics, Warrandale, PA, Nov. 1981, pp. 227-231.

7. Kelley, F. S.: Mesh Requirements of a Stress Concentration by the Specified Boundary Displacement Method. Proceedings of the Second International Computers in Engineering Conference, ASME, Aug. 1982, pp. 39-42.

8. Griffin, O. Hayden, Jr.; and Vidussoni, Marco A.: Global/Local Finite Element Analysis of Composite Materials. Computer–Aided Design in Composite Material Technology, C. A. Brebbia, W. P. de Wikle, and W. R. Blain (editors), Proceedings of the International

Conference for Computer–Aided Design in Composite Material Technology, Southampton, UK, April 13-15, 1988, pp. 513-524.

9. Jara-Almonte, C. C.; and Knight, C. E.: The Specified Boundary Stiffness/Force SBSF Method for Finite Element Subregion Analysis. International Journal for Numerical Methods in Engineering, Vol. 26, 1988, pp. 1567-1578.

10. Hirai, Itio; Wang, Bo Ping; and Pilkey, Walter D.: An Efficient Zooming Method for Finite Element Analysis. International Journal for Numerical Methods in Engineering, Vol. 20, 1984, pp. 1671-1683.

11. Hirai, Itio; Wang, Bo Ping; Pilkey, Walter D.: An Exact Zooming Method. Finite Element Analysis and Design, Vol. 1, No. 1, April 1985, pp. 61-68.

12. Dong, Stanley B.: Global–Local Finite Element Methods. State-Of-The-Art Surveys on Finite Element Technology, A. K. Noor and W. D. Pilkey (editors), ASME, 1983, pp. 451-474.

13. Stehlin, P.; and Rankin, C. C.: Analysis of Structural Collapse by the Reduced Basis Technique Using a Mixed Local–Global Formulation. AIAA Paper No. 86-0851-CP, May 1986.

14. Gladwell, G. M. L.: Practical Approximation Theory, University of Waterloo Press, 1974.

15. Harder, Robert L.; and Desmarais, Robert N.: Interpolation Using Surface Splines. Journal of Aircraft, Vol. 9, No. 2, February 1972, pp. 189-191.

16. Stewart, Caroline B., Compiler: The Computational Structural Mechanics Testbed User's Manual. NASA TM–100644, 1989.

17. Gillian, R. E.; and Lotts, C. G.: The CSM Testbed Software System – A Development Environment for Structural Analysis Methods on the NAS CRAY–2. NASA TM–100642 , 1988.

18. Timoshenko, S. P.; and Goodier, J. N.: Theory of Elasticity. McGraw–Hill Book Company, New York, 1934, pp. 90-97.

19. Peterson, R. E.: Stress Concentration Design Factors. Wiley-International, New York, 1953, pp. 77-88.

20. Almroth, B. O.; and Brogan, F. A.: The STAGS Computer Code. NASA CR–2950, 1978.

21. Almroth, B. O.; Brogan, F. A.; and Stanley, G. M.: Structural Analysis of General Shells - Volume II: User Instructions for STAGSC-1. NASA CR-165671, 1981.

22. Starnes, James H., Jr.; Dickson, John N.; and Rouse, Marshall: Postbuckling Behavior of Graphite–Epoxy Panels. ACEE Composite Structures Technology: Review of Selected NASA Research on Composite Materials and Structures. NASA CP–2321, 1984, pp. 137-159.

23. Williams, Jerry G.; Anderson, Melvin S.; Rhodes, Marvin D.; Starnes, James H., Jr.; and Stroud, W. Jefferson: Recent Developments in the Design, Testing, and Impact–Damage Tolerance of Stiffened Composite Panels. NASA TM–80077, 1979.

24. Knight, Norman F., Jr.; McCleary, Susan L.; Macy, Steven C.; and Aminpour, Mohammad A.: Large–Scale Structural Analysis: The Structural Analyst, The CSM Testbed, and The NAS System. NASA TM–100643, 1989.

Table 1 Finite Element Models of Isotropic Panel with Circular Cutout.

Model Designation	Number of Rings of Nodes	Number of Radial Spokes of Elements	Total Number of Elements	Total Number of Nodes	K_t
G1	2	16	256	296	2.06
G2	4	16	288	328	2.23
G3	16	32	832	888	2.72
G4[a]	32	80	3168	3272	2.81
LS1	16	32	512	544	2.76
LC1	16	32	512	544	2.75

[a] G4 is the converged model

Table 2 Summary of Computational Requirements.

Model Designation	Measures of Computational Effort		
	Total number of degrees of freedom	CPU, seconds	Size of data library, Mbytes
G1	1644	64.0	5.2
G2	1836	69.7	6.0
G3	5156	183.4	22.2
G4[a]	19340	1167.2	160.0
LS1	3072	135.4	13.0
LC1	3072	121.6	12.6

[a] G4 is the converged model

Table 3 Finite Element Models Blade–Stiffened Panel with Discontinuous Stiffener.

Model Designation	Number of Rings of Nodes	Number of Radial Spokes of Elements	Total Number of Elements	Total Number of Nodes	$\frac{(N_x)_{max}}{(N_x)_{avg}}$
G1	2	16	376	424	2.22
G2	16	32	1024	1088	2.88
G3	16	32	1408	1488	2.88
G4[a]	32	80	3472	3584	2.94
LC1	16	32	576	612	2.92
LR1	-	-	16	25	-
LR2	-	-	32	45	-
LR3	-	-	96	117	-

[a] G4 is the converged model

Table 4 Summary of Computational Requirements.

Model Designation	Measures of Computational Effort		
	Total number of degrees of freedom	CPU, seconds	Size of data library, Mbytes
G1	2316	99.7	8.7
G2	6252	255.3	28.9
G3	8460	329.6	38.5
G4[a]	21084	1006.0	140.6
LC1	3456	188.7	13.1
LR1	54	58.0	0.5
LR2	126	62.0	0.8
LR3	462	78.7	1.8

[a] G4 is the converged model

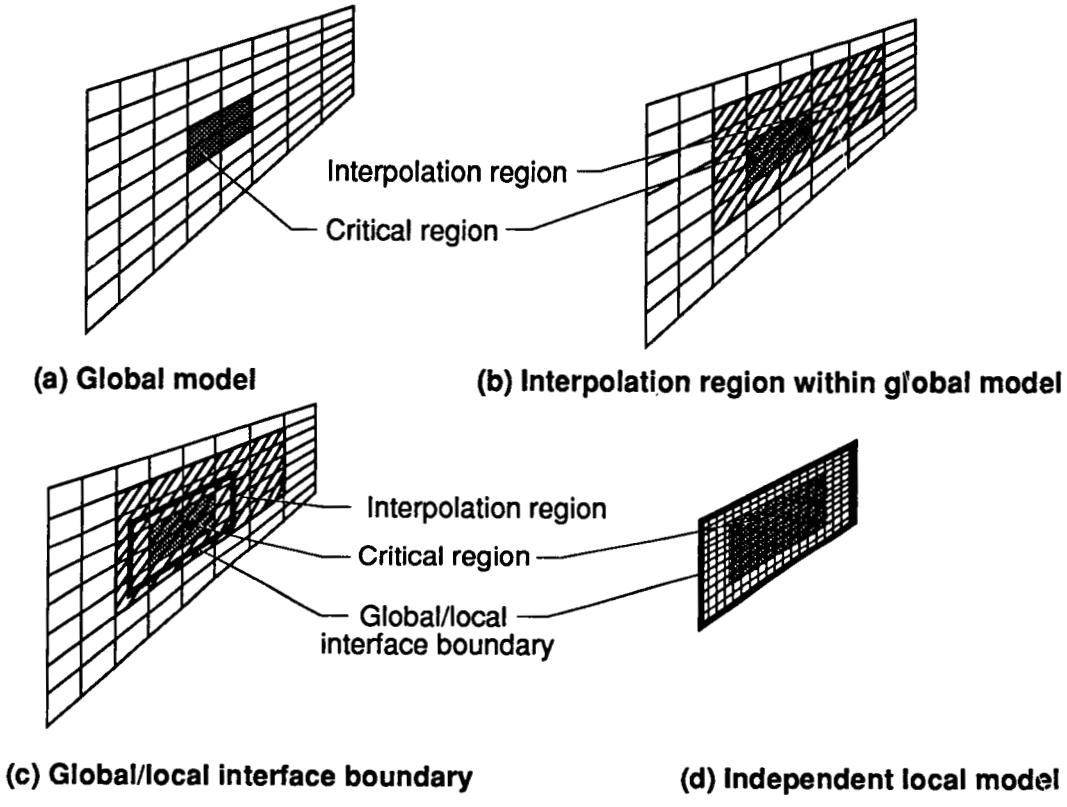

Fig. 1 Terminology of the global/local methodology.

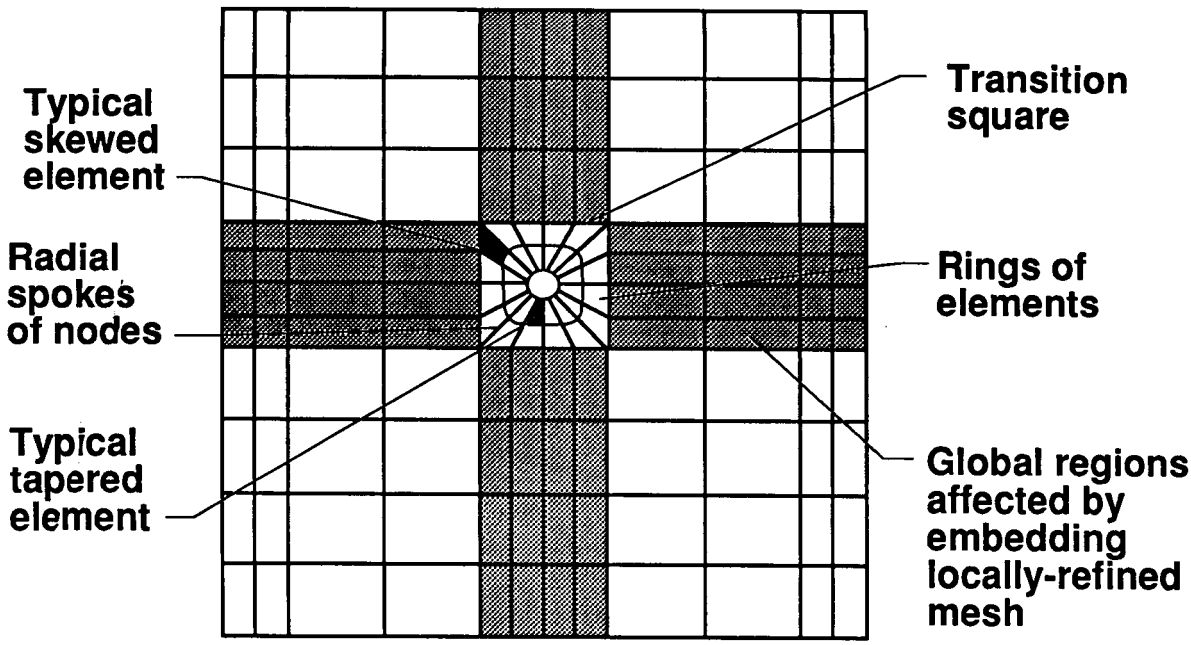

Fig. 2 Terminology associated with modeling cutouts.

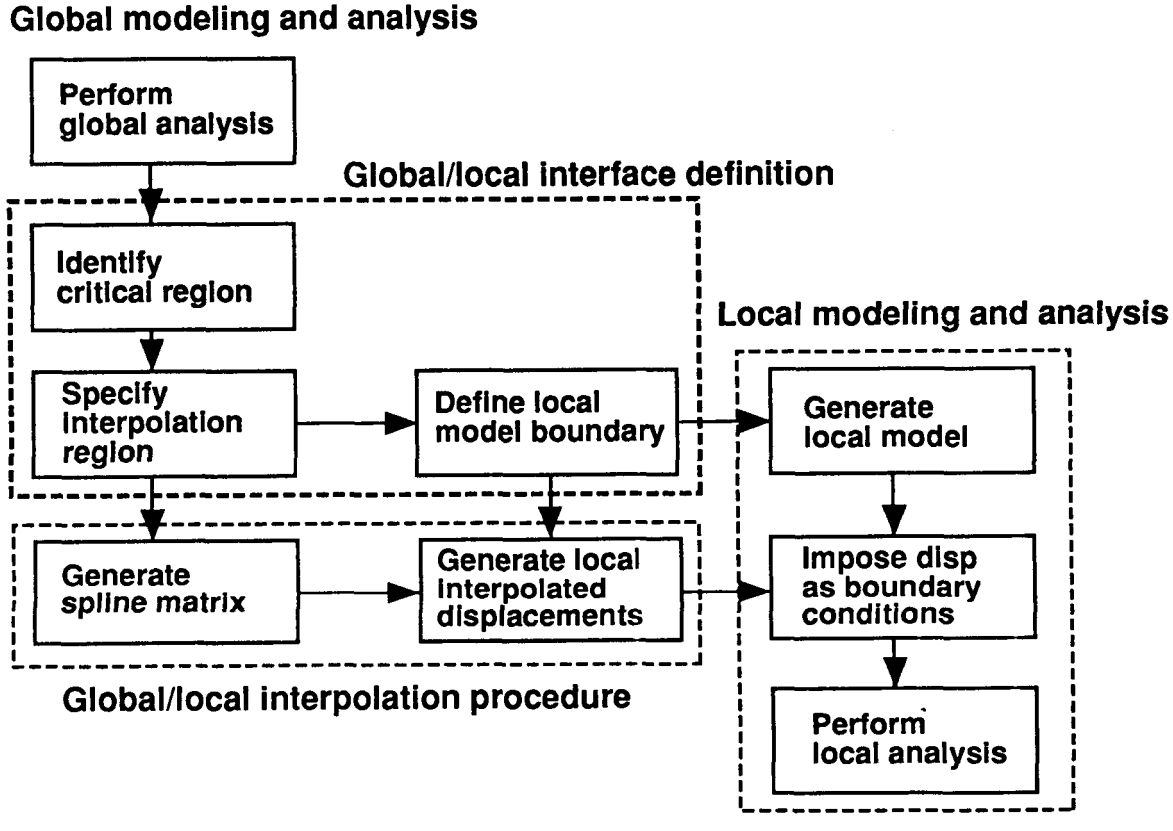

Fig. 3 Schematic of overall global/local solution strategy.

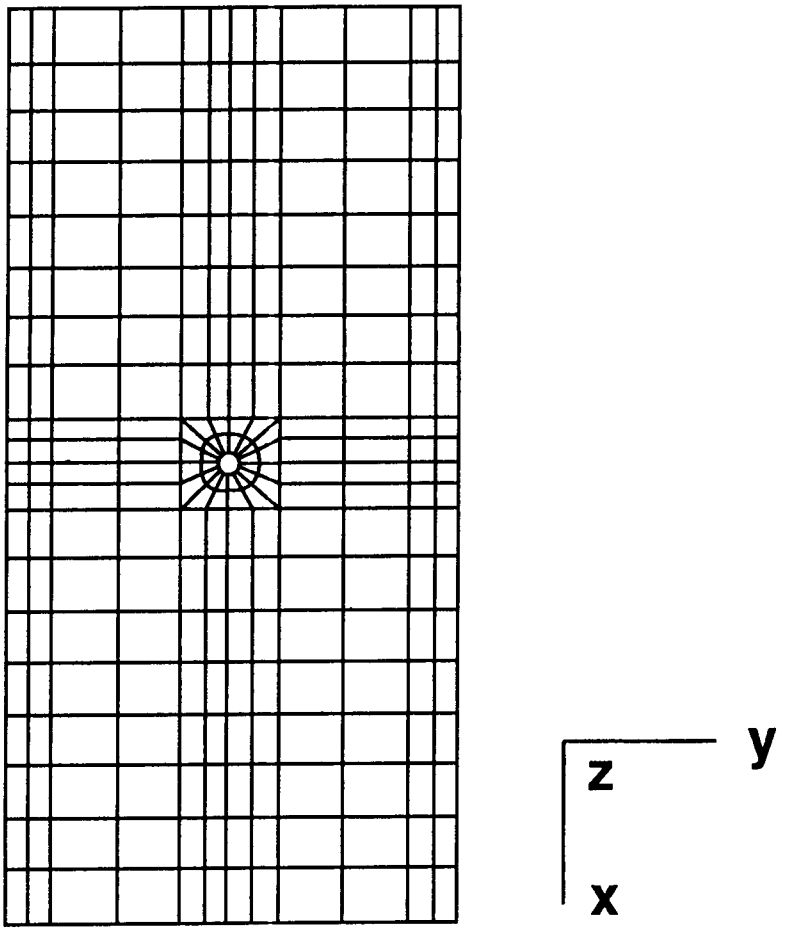

Fig. 4 Coarse global finite element model of isotropic panel with a circular cutout.

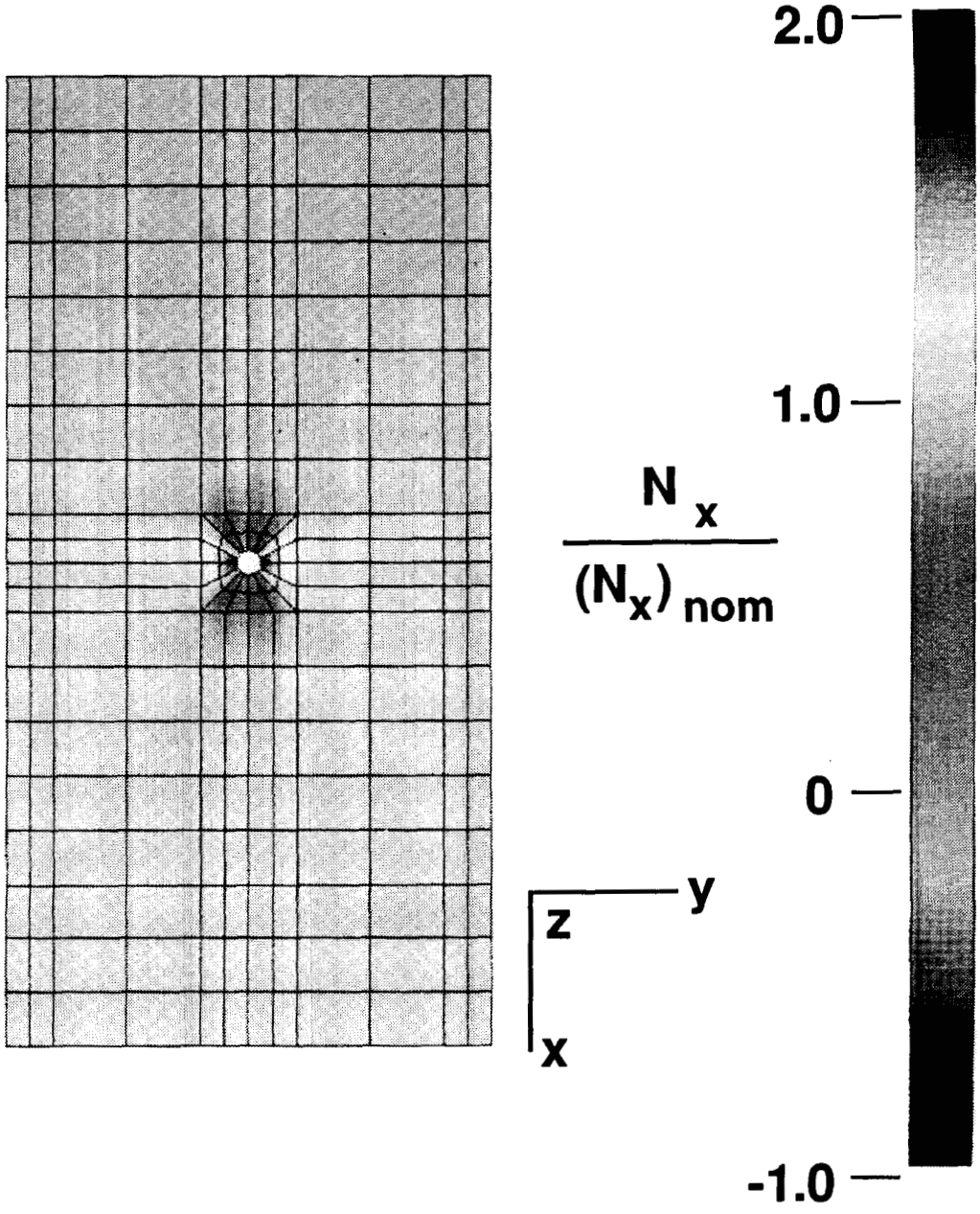

Fig. 5 Longitudinal stress resultant N_x distribution for coarse global finite element model of isotropic panel with a circular cutout.

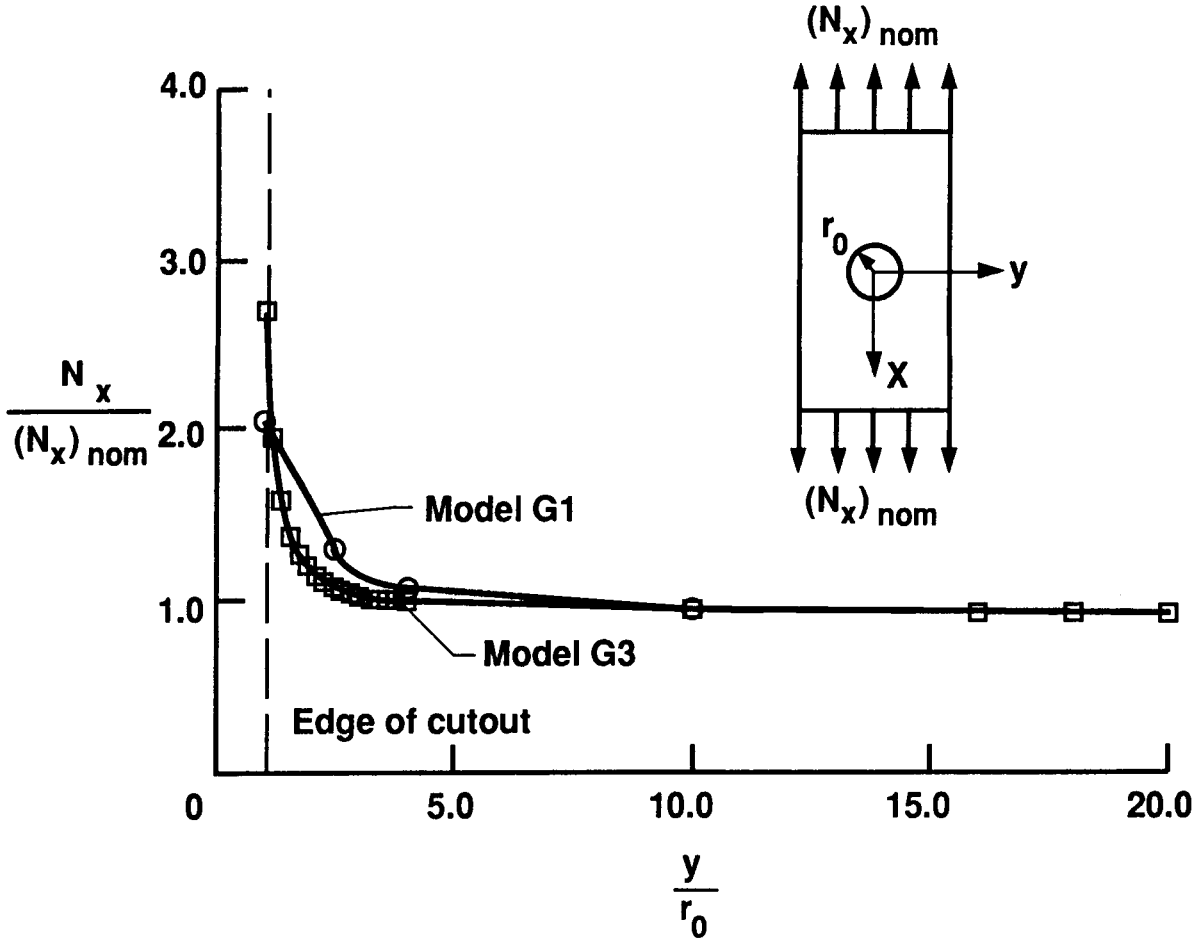

Fig. 6 Longitudinal inplane stress resultant N_x distributions at panel midlength for coarse and refined global finite element models

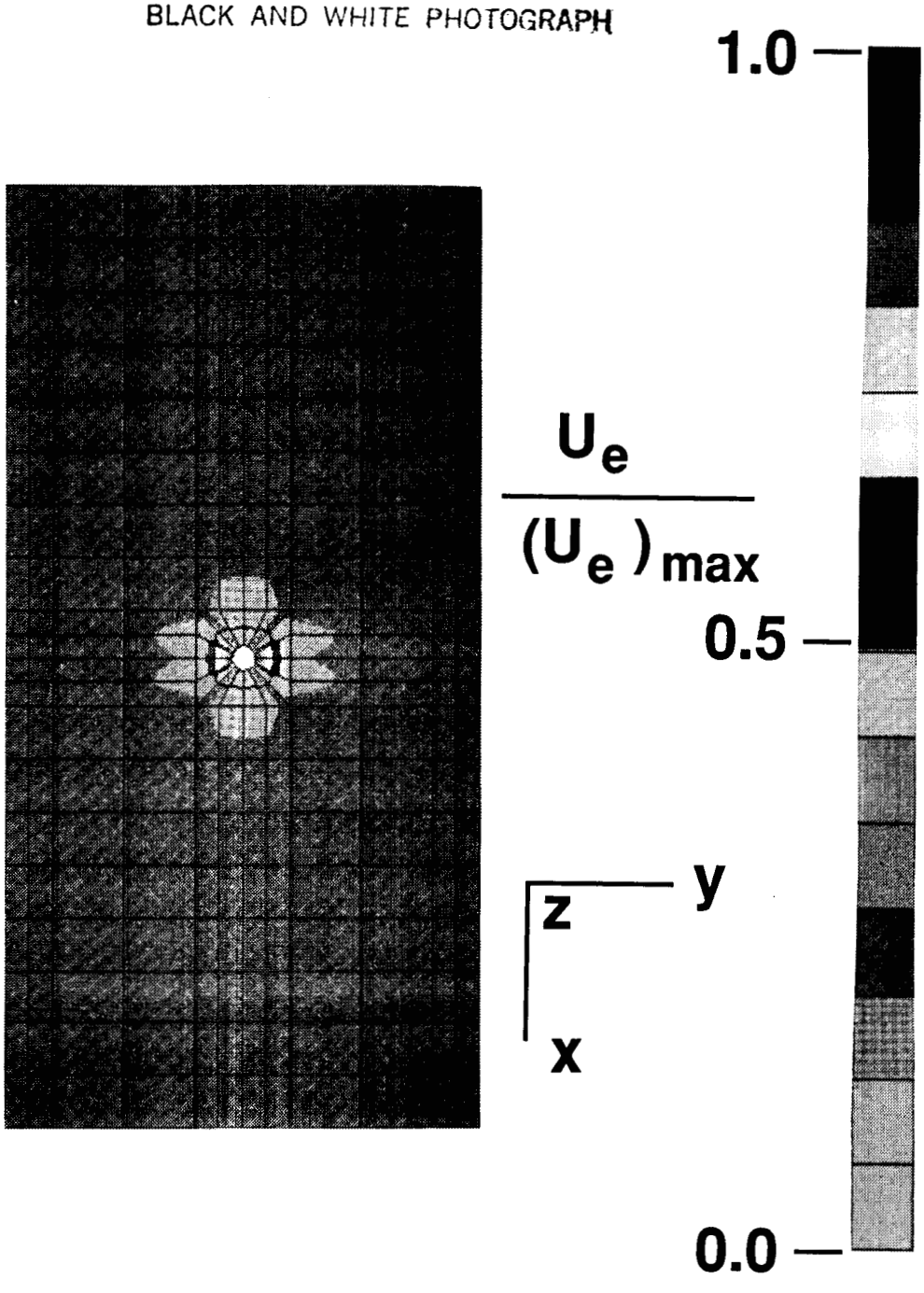

Fig. 7 Distribution of the strain energy measure for coarse global model of the panel with a circular cutout.

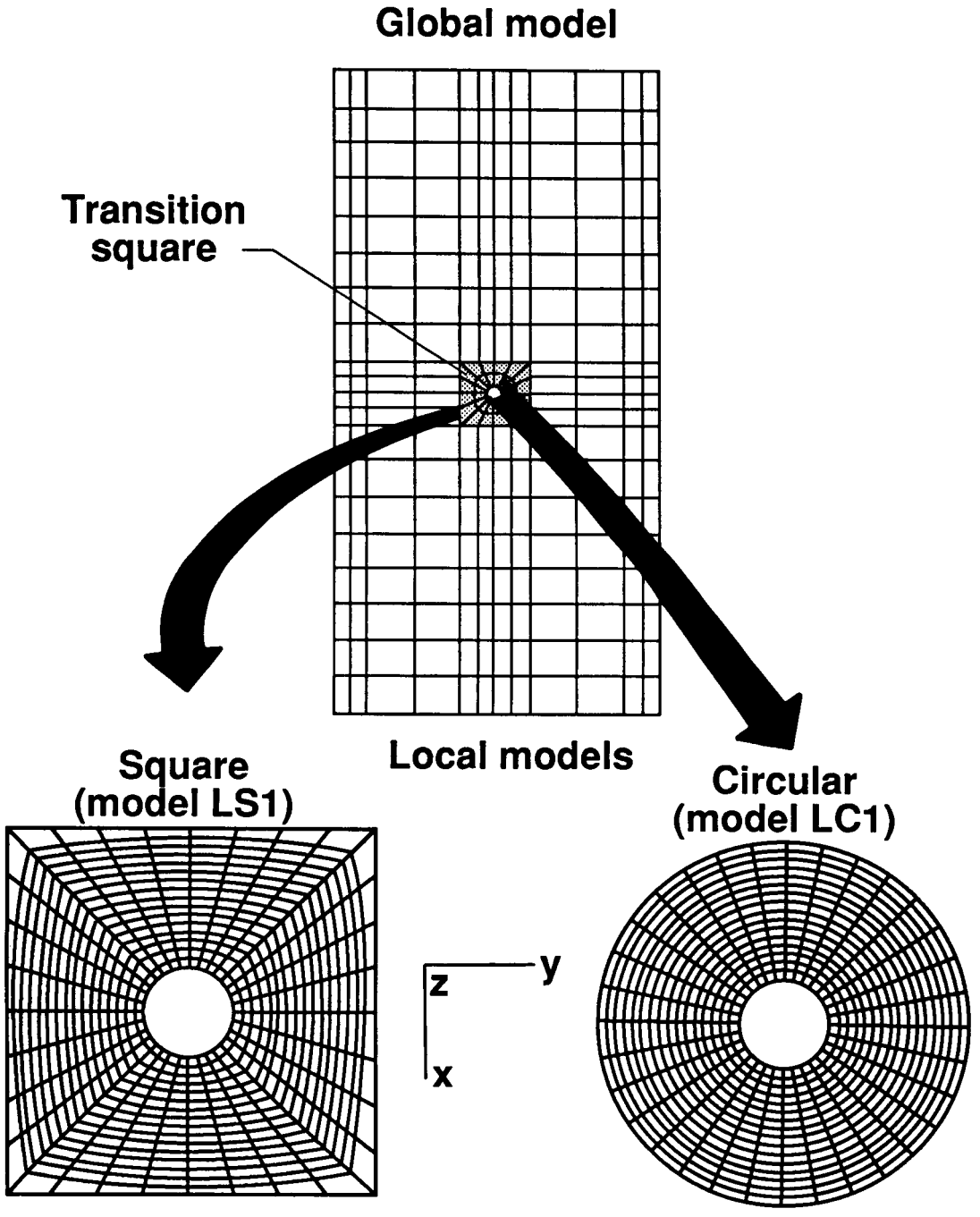

Fig. 8 Global/local analysis models for isotropic panel with circular cutout.

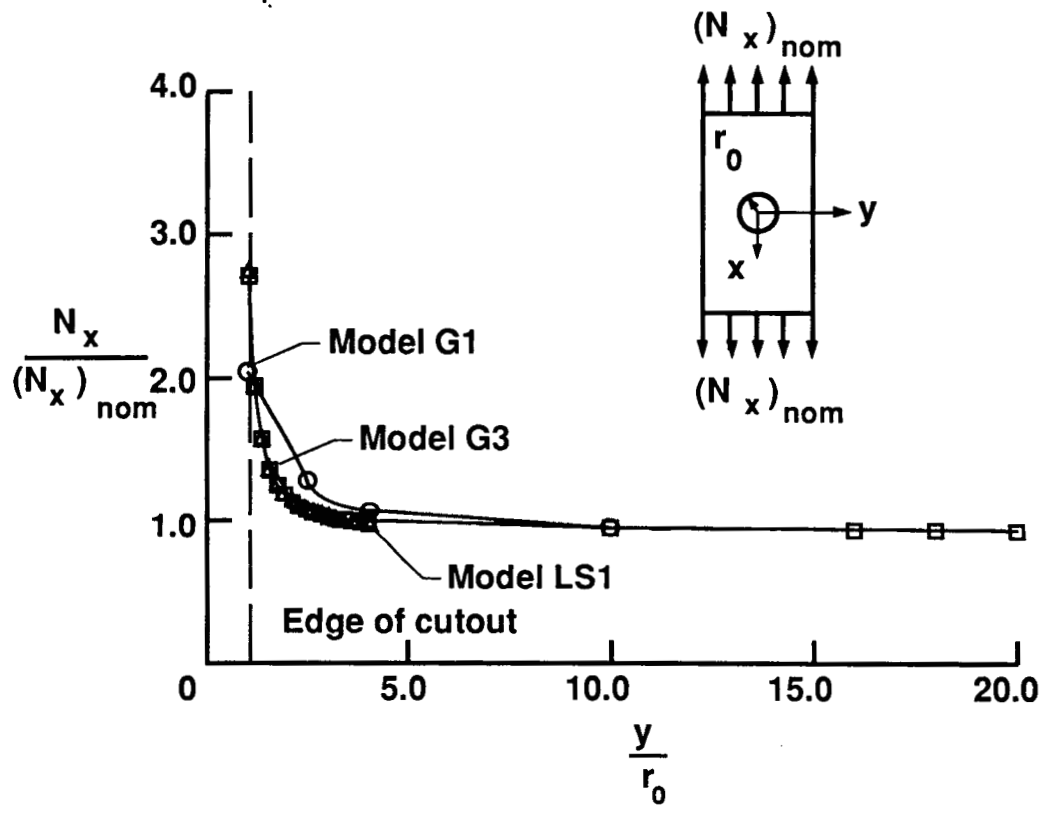

(a) Distribution at panel midlength.

Fig. 9 Longitudinal stress resultant N_x distributions for square local finite element model of isotropic panel with a circular cutout.

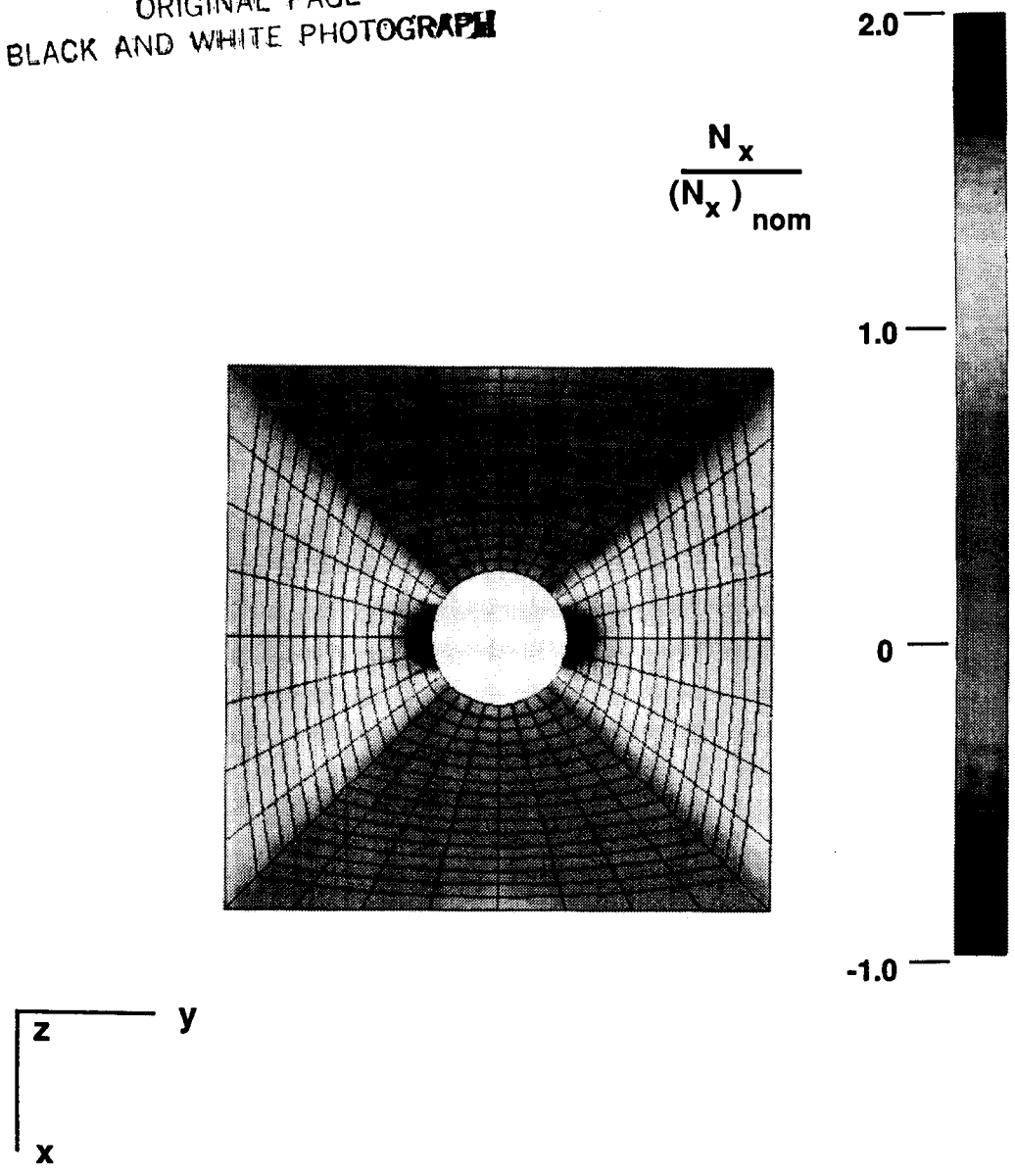

(b) Contour plot.

Fig. 9 Concluded.

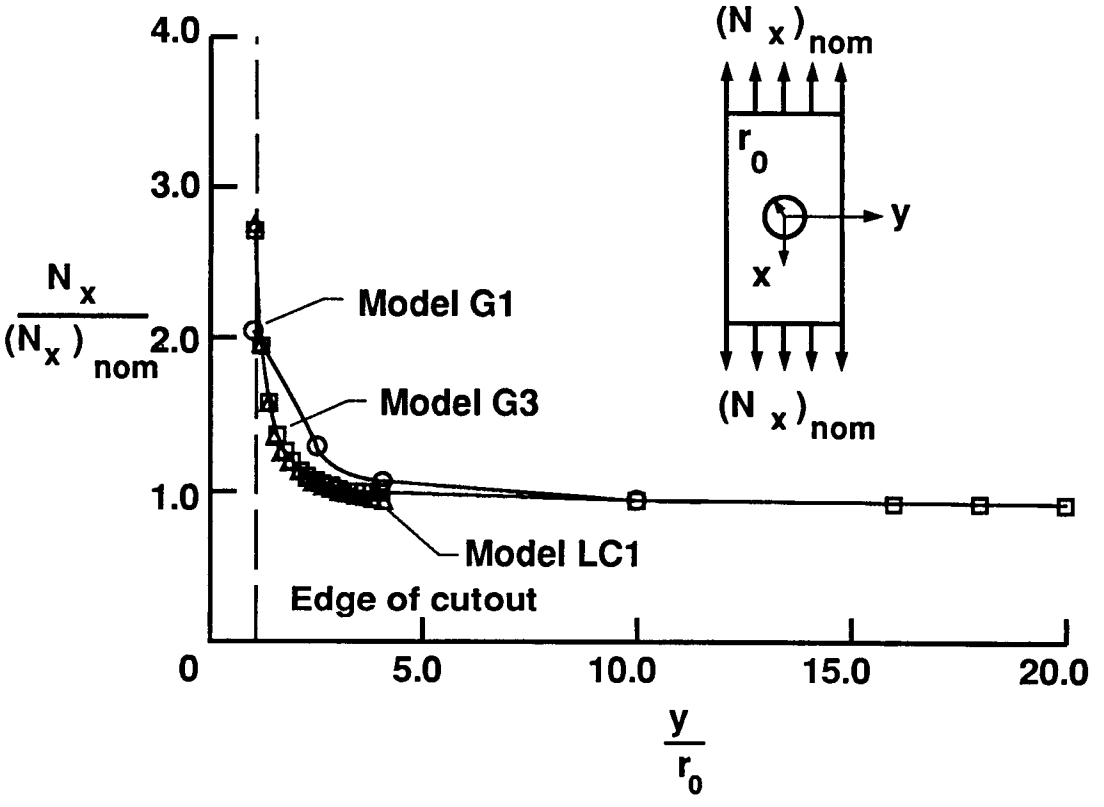

(a) Distribution at panel midlength.

Fig. 10 Longitudinal stress resultant N_x distributions for circular local finite element model of isotropic panel with a circular cutout.

ORIGINAL PAGE
BLACK AND WHITE PHOTOGRAPH

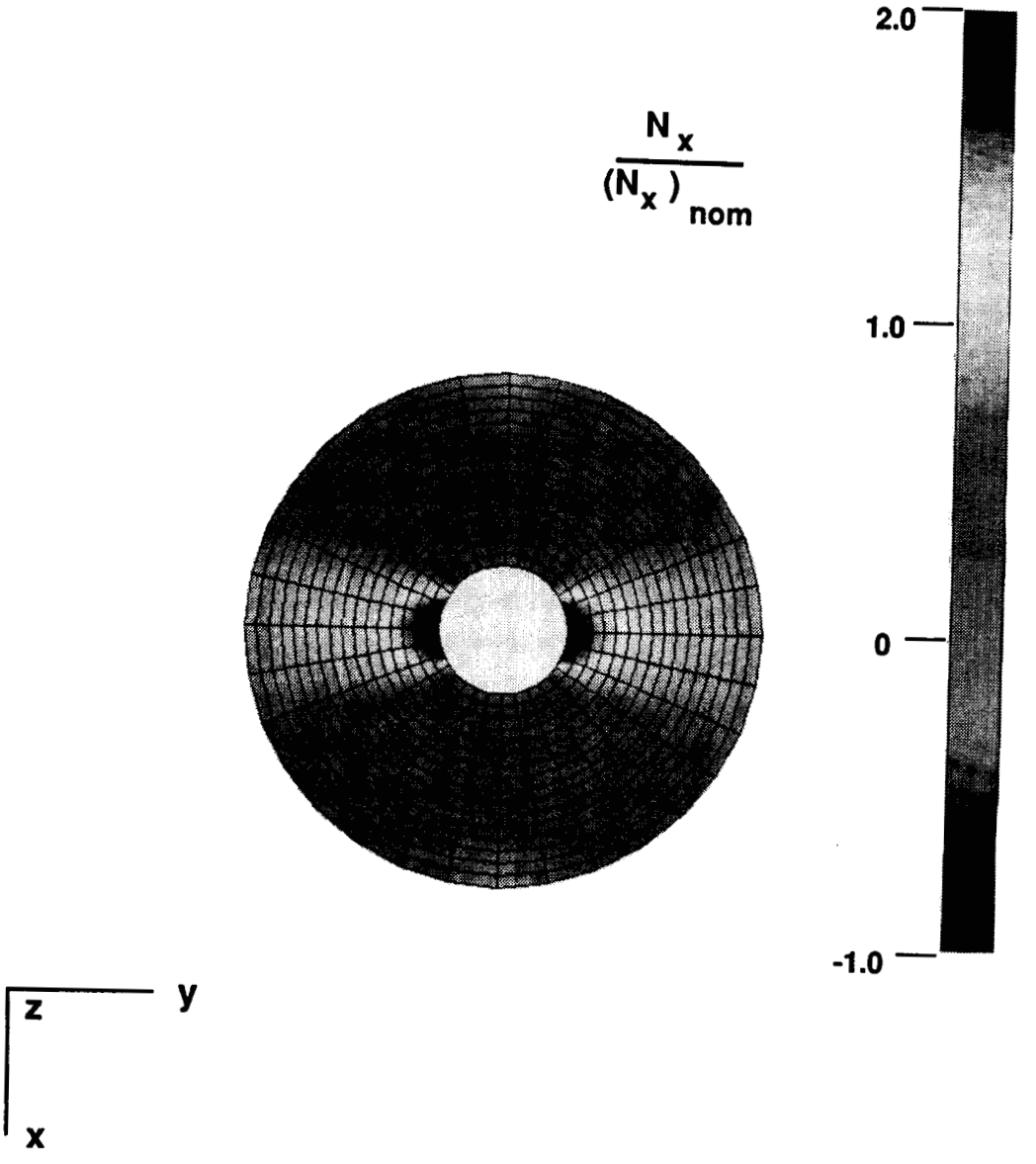

(b) Contour plot.

Fig. 10 Concluded.

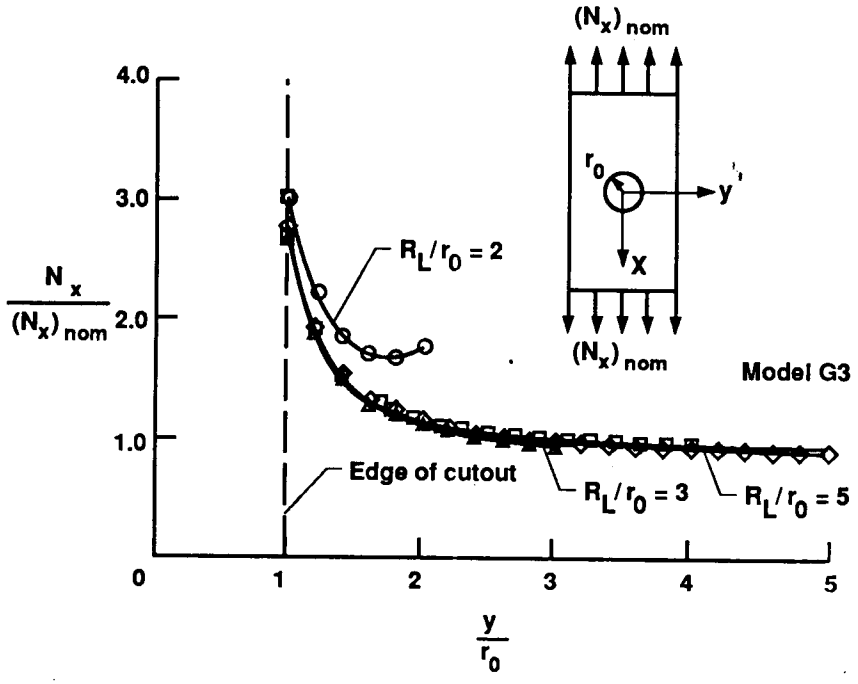

(a) Interpolation from global Model G1.

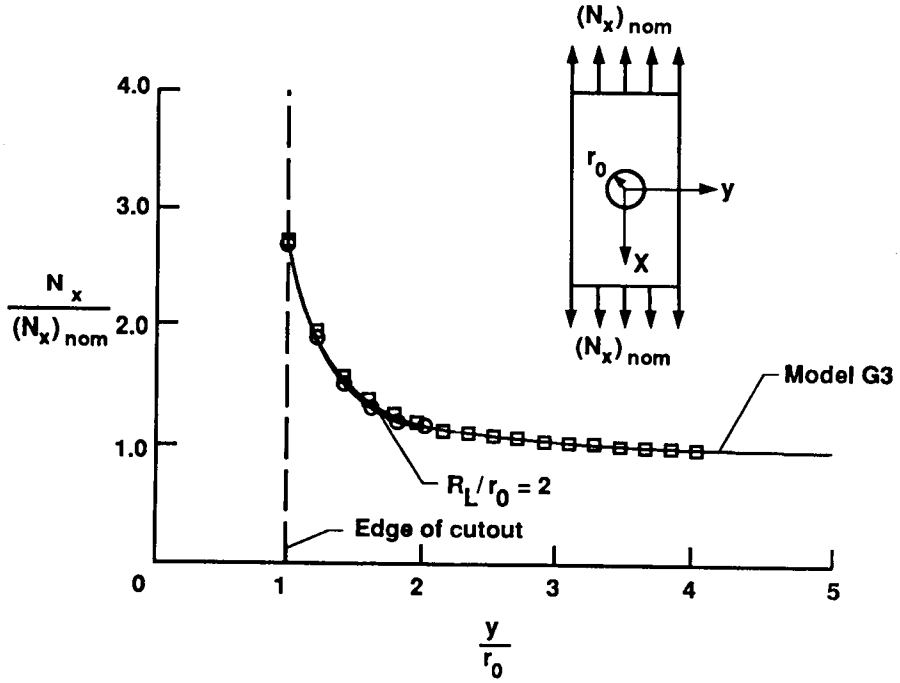

(b) Interpolation from global Model G2.

Fig. 11 Longitudinal inplane stress resultant N_x distributions at panel midlength for varied local model boundaries.

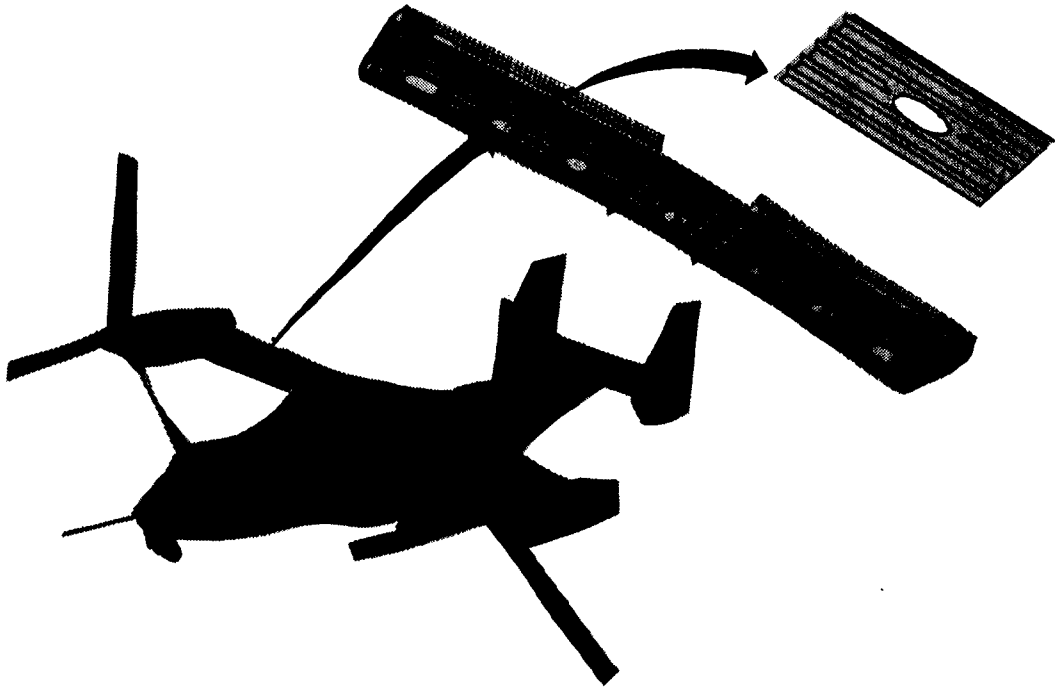

Fig. 12 Bell–Boeing V–22 wing panel.

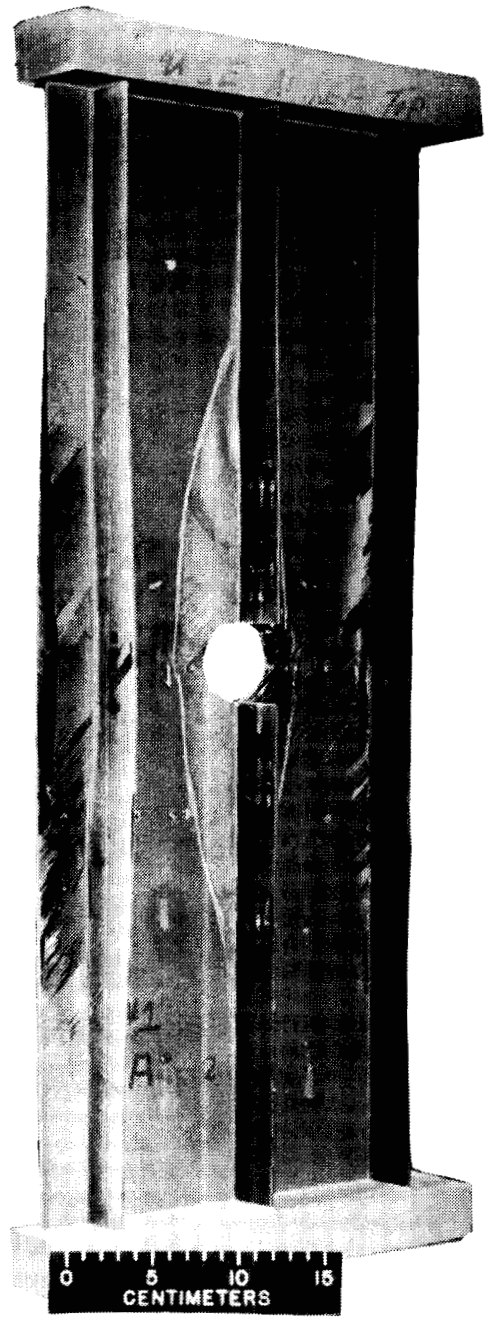

13 Composite blade–stiffened panel with a discontinuous stiffener.

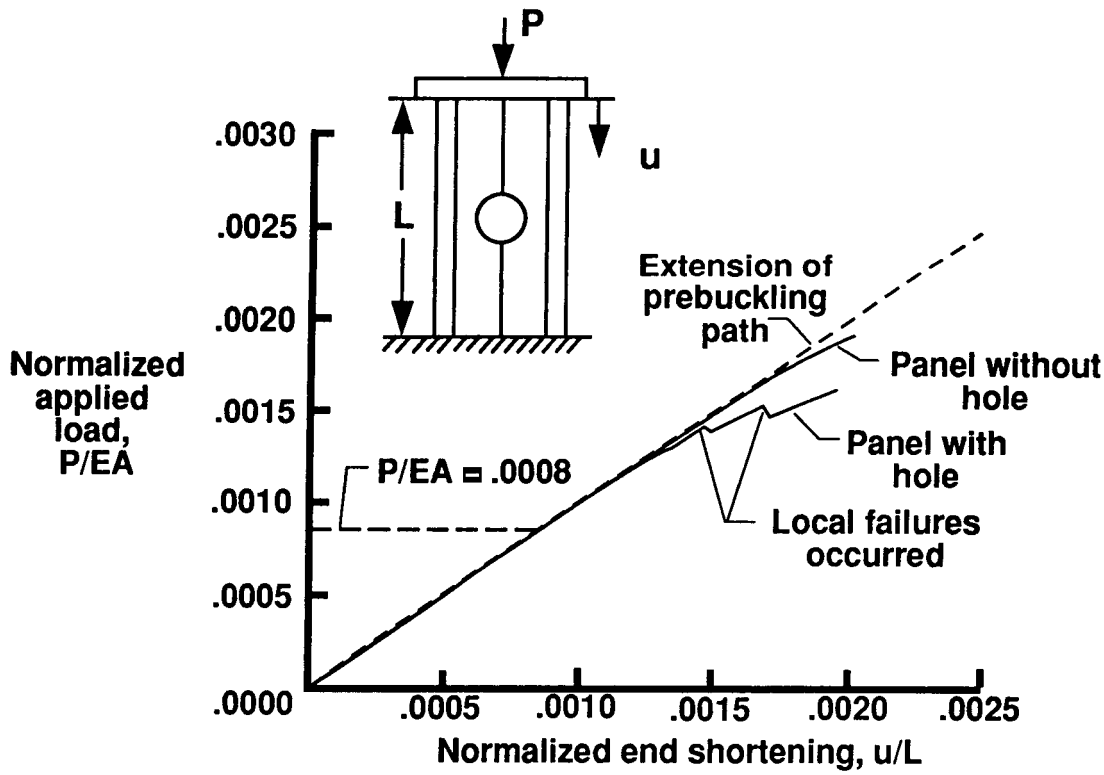

Fig. 14 End–shortening results for composite blade–stiffened panel.

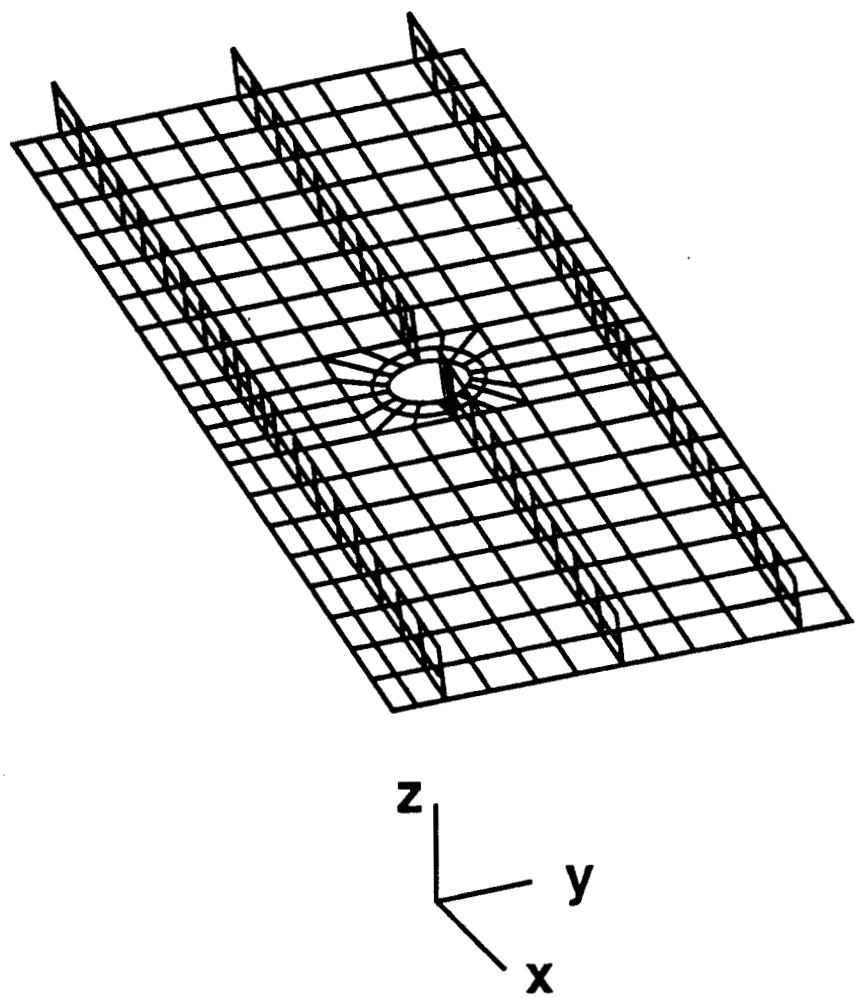

Fig. 15 Global finite element model of blade–stiffened panel with discontinuous stiffener.

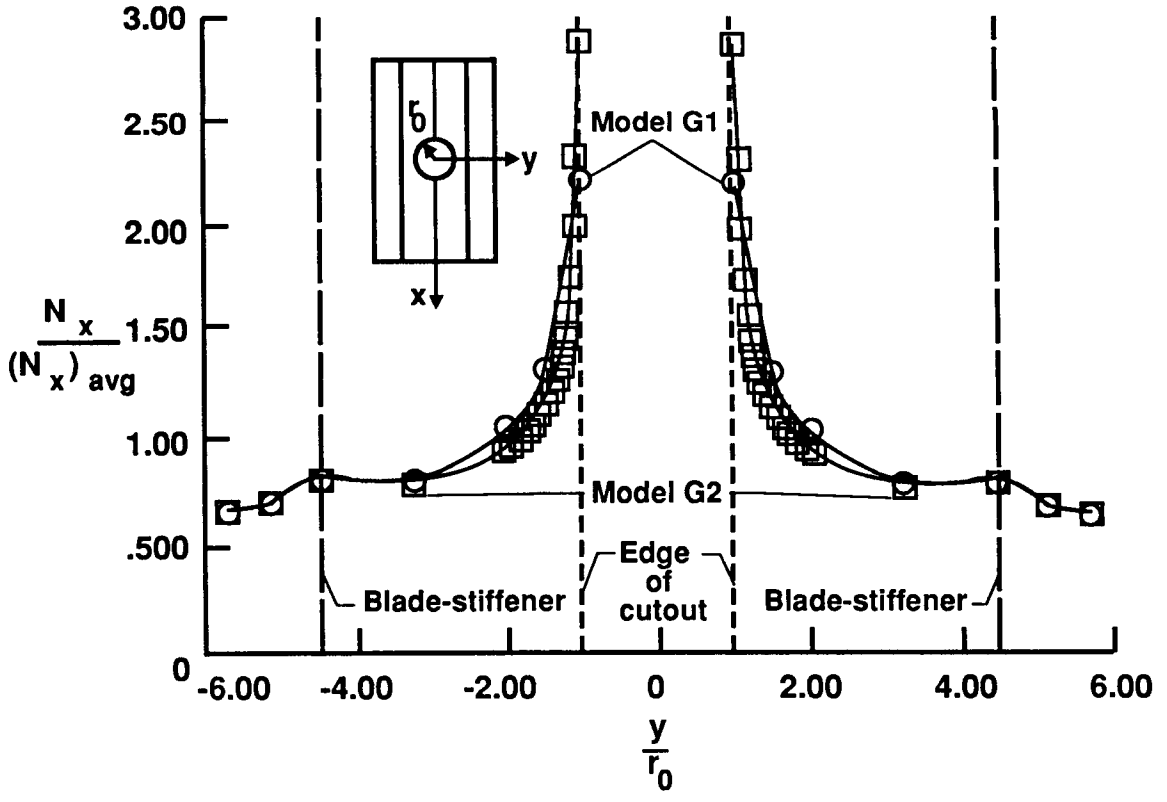

Fig. 16 Longitudinal inplane stress resultant N_x distributions at panel midlength for coarse and refined global models.

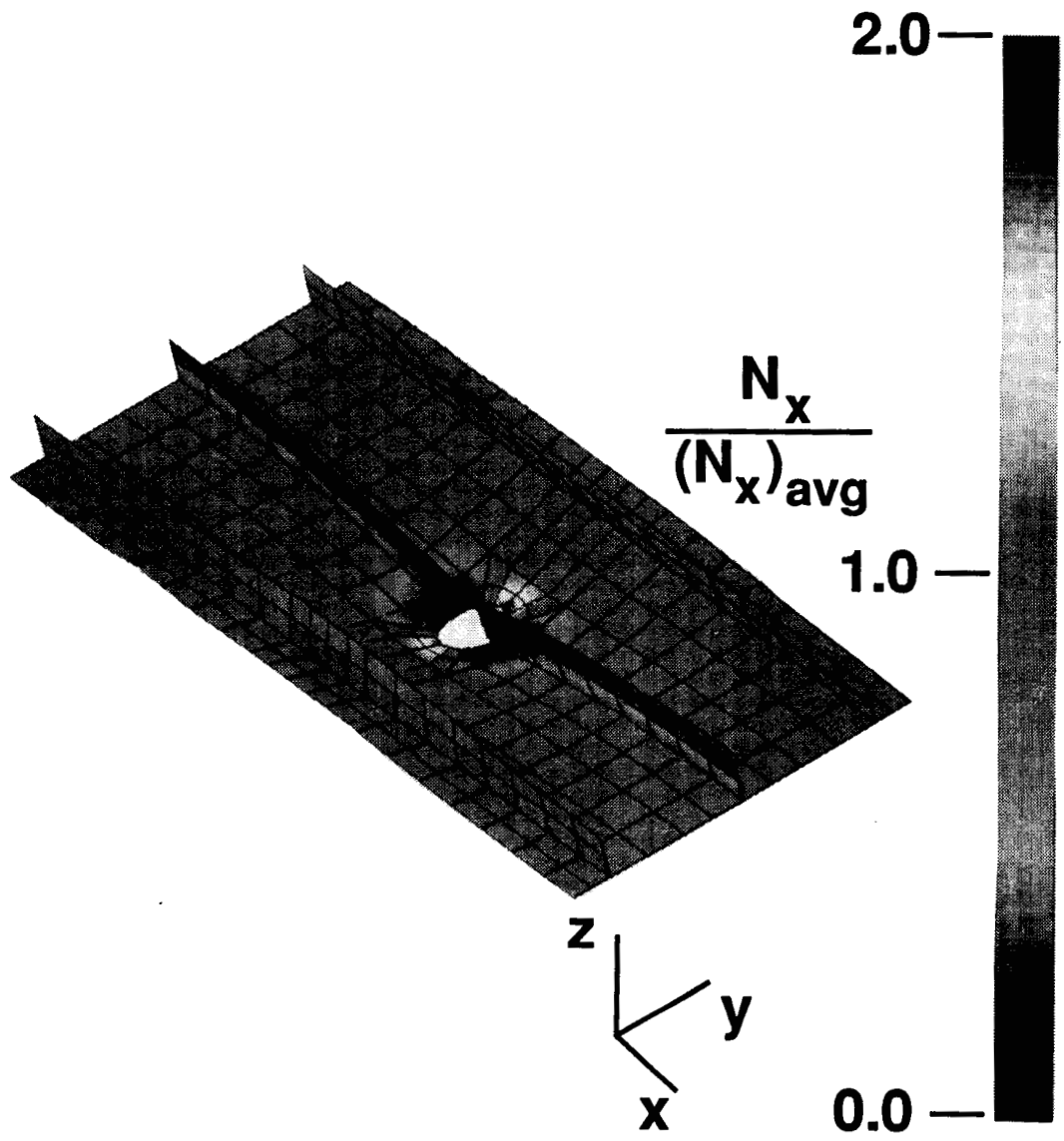

Fig. 17 Deformed geometry shape with N_x distributions for coarse global model of blade–stiffened panel with discontinuous stiffener.

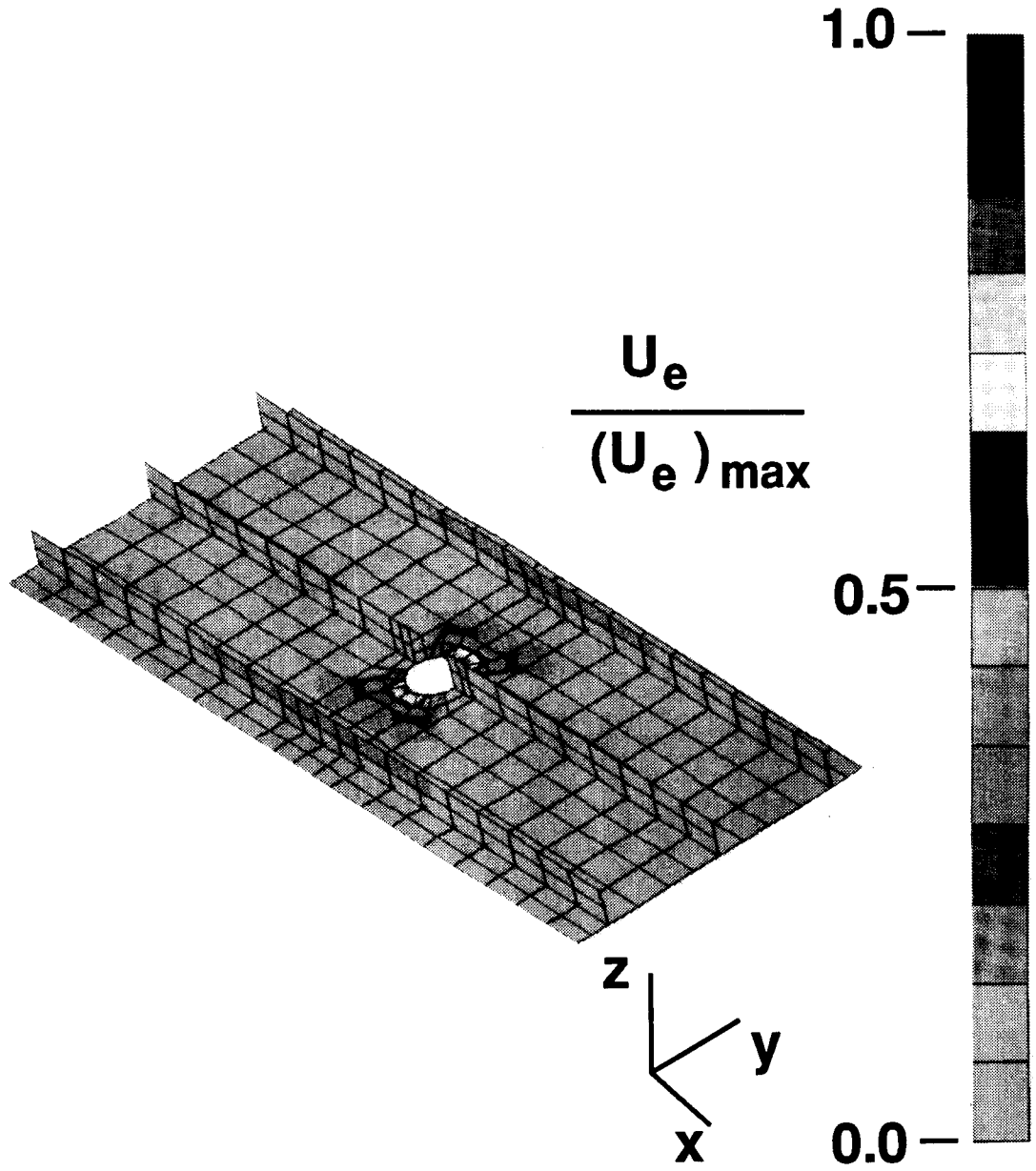

Fig. 18 Distribution of the strain energy measure for the coarse model of the blade–stiffened panel with discontinuous stiffener.

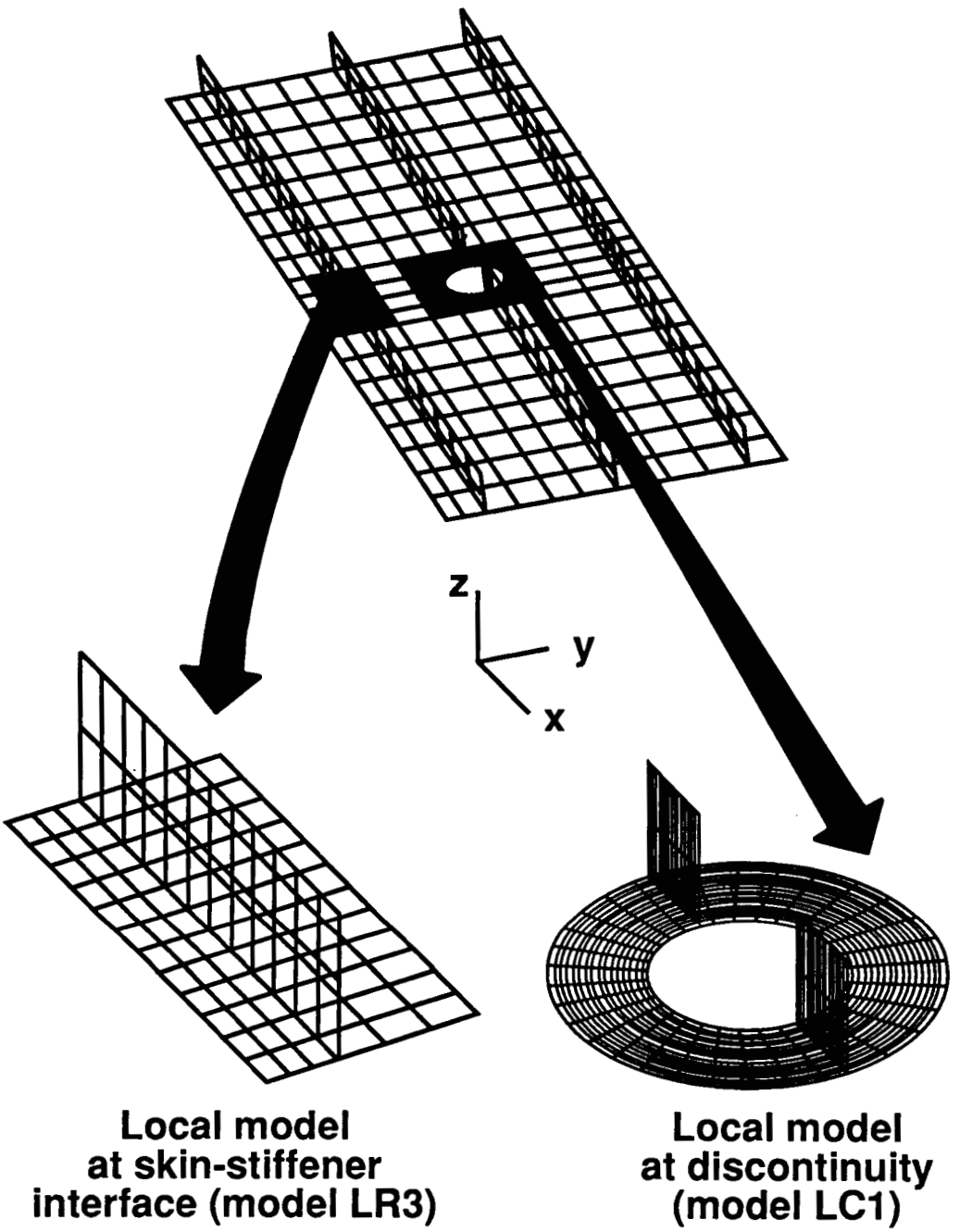

Fig. 19 Global/local analysis models for blade–stiffened panel with discontinuous stiffener.

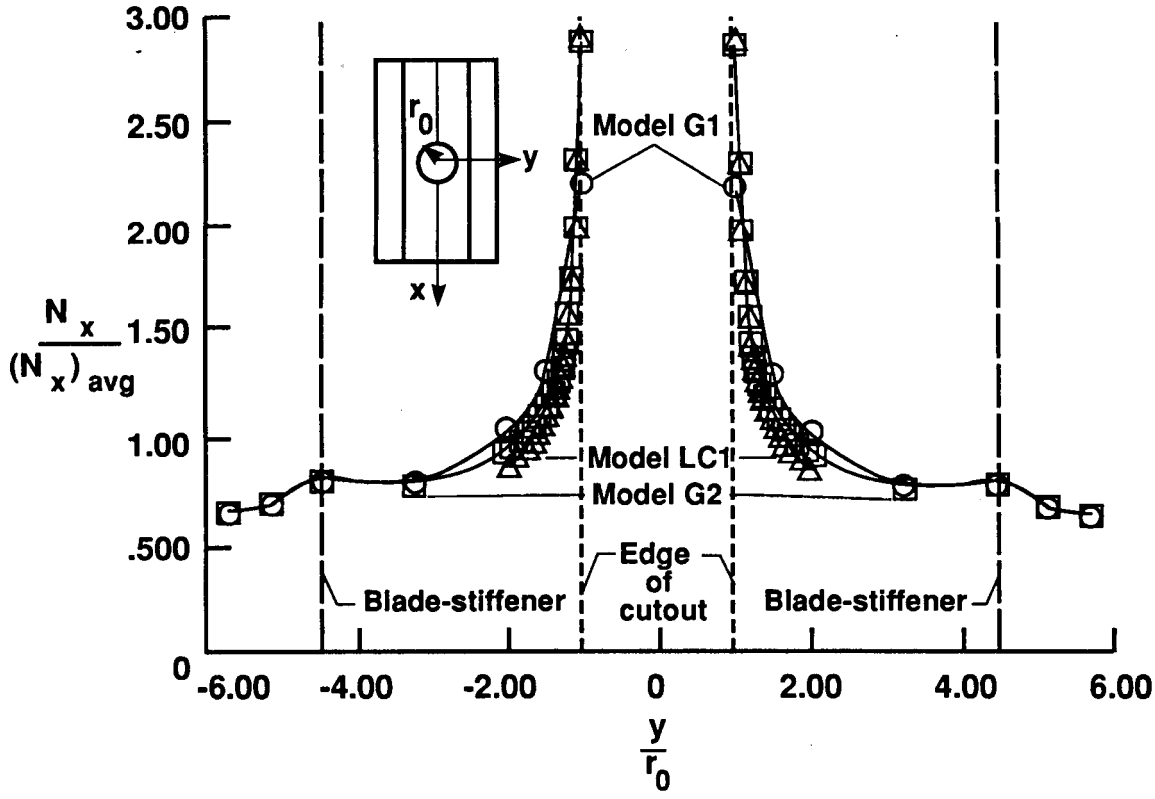

(a) Distribution at panel midlength.

Fig. 20 Longitudinal stress resultant N_x distributions for circular local finite element model of blade–stiffened panel with discontinuous stiffener.

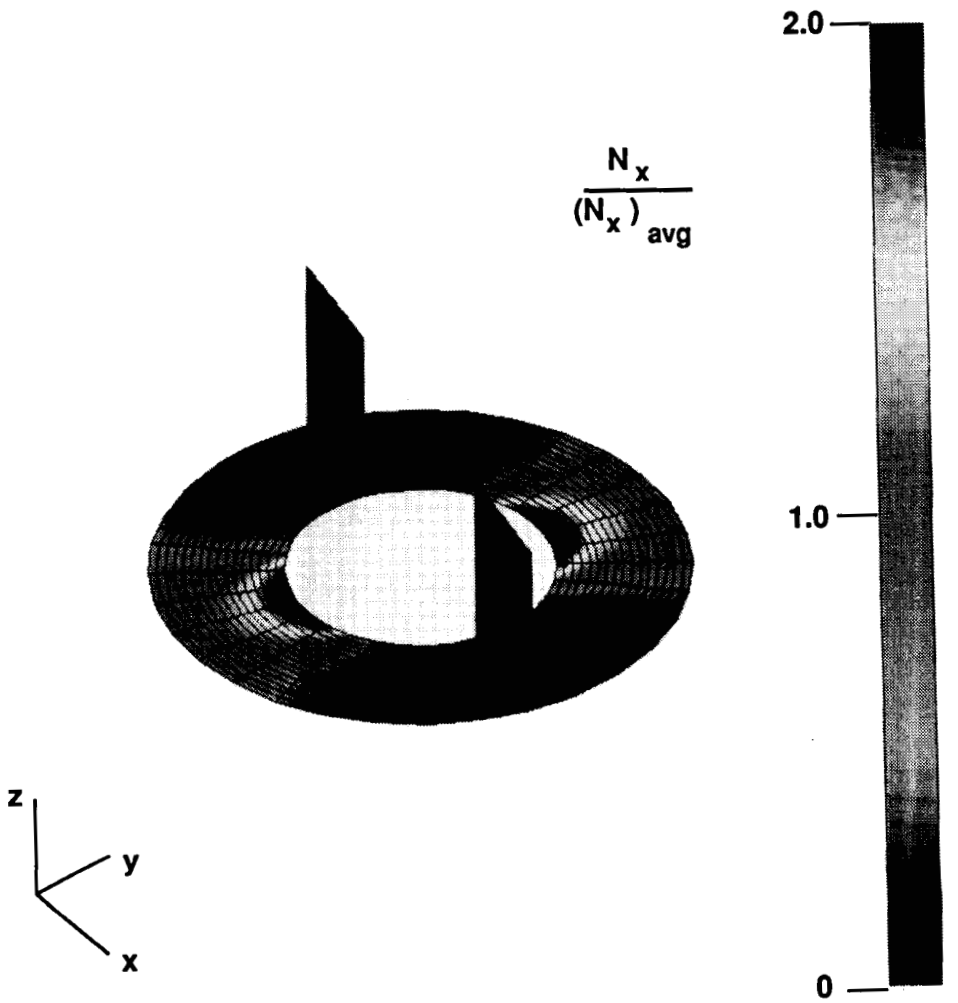

(b) Contour plot.

Fig. 20 Concluded.

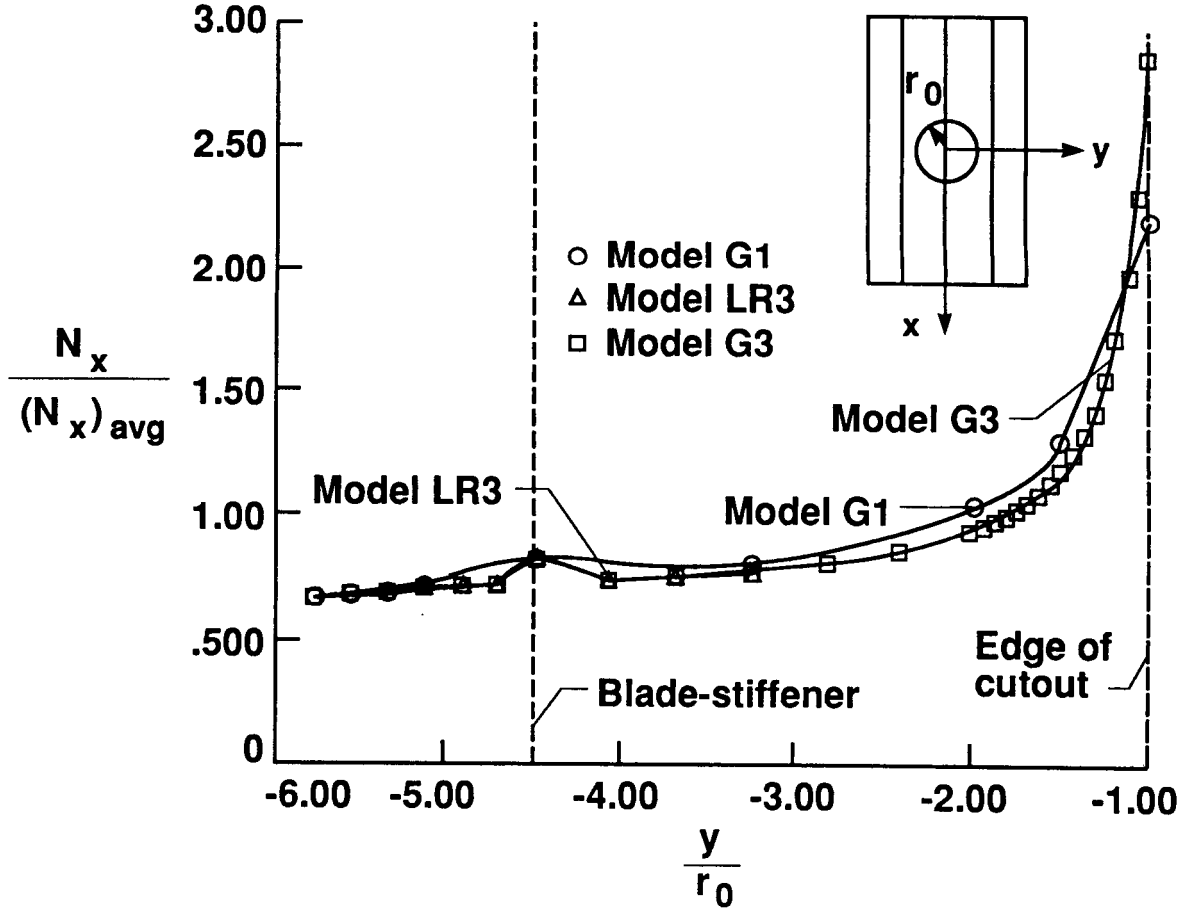

Fig. 21 Longitudinal inplane stress resultant N_x distributions at panel midlength for skin-stiffener interface region.

NASA
National Aeronautics and Space Administration

Report Documentation Page

1. Report No.	2. Government Accession No.	3. Recipient's Catalog No.
NASA TM-101622		

4. Title and Subtitle	5. Report Date
Global/Local Stress Analysis of Composite Panels	June 1989
	6. Performing Organization Code
7. Author(s)	8. Performing Organization Report No.
Jonathan B. Ransom and Norman F. Knight, Jr.	
9. Performing Organization Name and Address	10. Work Unit No.
NASA Langley Research Center Hampton, VA 23665-5225	505-63-01-10
	11. Contract or Grant No.
12. Sponsoring Agency Name and Address	13. Type of Report and Period Covered
National Aeronautics and Space Administration Washington, DC 20546-0001	Technical Memorandum
	14. Sponsoring Agency Code

15. Supplementary Notes

Presented at the Third Joint ASCE/ASME Mechanics Conference, University of California at San Diego, July 9-12, 1989.

16. Abstract

A method for performing a global/local stress analysis is described and its capabilities are demonstrated. The method employs spline interpolation functions which satisfy the linear plate bending equation to determine displacements and rotations from a global model which are used as "boundary conditions" for the local model. Then, the local model is analyzed independent of the global model of the structure. This approach can be used to determine local, detailed stress states for specific structural regions using independent, refined local models which exploit information from less-refined global models. The method presented is not restricted to having a priori knowledge of the location of the regions requiring local detailed stress analysis. This approach also reduces the computational effort necessary to obtain the detailed stress state. Criteria for applying the method are developed. The effectiveness of the method is demonstrated using a classical stress concentration problem and a graphite-epoxy blade-stiffened panel with a discontinuous stiffener.

17. Key Words (Suggested by Authors(s))	18. Distribution Statement
Global/Local Analysis Detailed Stress Analysis Computational Structural Mechanics Surface Splines	Unclassified—Unlimited Subject Category 39

19. Security Classif.(of this report)	20. Security Classif.(of this page)	21. No. of Pages	22. Price
Unclassified	Unclassified	53	A03

For sale by the National Technical Information Service, Springfield, Virginia 22161-2171